uc3m | Universidad Carlos III de Madrid

Aerospace Engineering
2016/2017

Bachelor Thesis

Numerical study of the behavior against impact of personal protections

---

Álvaro Dosantos Moreno

Tutor
Carlos Santiuste Romero

Contents

List of Tables

List of Figures

1 Introduction

1.1 Motivation

As weaponry modernizes and gets more powerful, defense systems also have to be adapted and developed to counter this. In the US more than 11,500 people are killed with guns each year [7][8] and every armed conflict has casualties. For example the war in Afghanistan has claimed the lives of 2,386 soldiers only in the US side[9] and more than 20,000 in the afghan side [10]. Surely some of these deaths could have been avoided with a better type of body armor.

Another important reason to keep on developing personal protections is due to the terrorism threat. An act of terrorism can be carried out anywhere with a wide array of weapons (shotguns, military rifles, explosives, machetes...) so the type of protection needs to be adapted to each threat.

This is being tackled by developing new materials, more resistant and lighter, which increase maneuverability, survivability and comfort.

The most important characteristic of body armor is its ballistic resistance. The higher it is, the most protection it can offer. Some types of protection are certified to resist a certain level of threat, if it is overcome, the armor will not protect its carrier.

To asses the ballistic capacity several methods can be used, using finite element models (e.g., Abaqus, CATIA, LS-DYNA) or experimental procedures. The models are also studied after failing, to discover why it happened and how to avoid this from happening.

The criteria used to evaluate ballistic materials are: density, yield strength, energy absorption and V_{50}, to name a few. The ballistic threats usually have high velocity, small mass, and ,in the case of explosions, irregular sized pellets (shrapnel).

The objective of personal protections is to absorb and dissipate the energy of the projectile in a non-lethal way for the user. Generally, this is achieved by distributing the energy on the point of impact over a wider area. This usually results in blunt trauma after being shot, as the bullet deforms, see Fig.1.

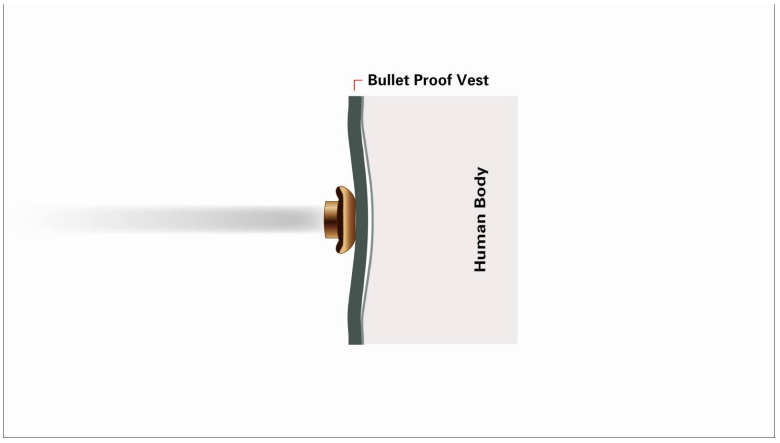

Figure 1: Deformation experienced by bullets after impact.

Testing protections for each type of threat, for each part of the body and for each kind of projectile is done experimentally, and this requires huge amounts of money and time. Every configuration of a protection has to be tested hundreds of times per type of projectile.

The simulations carried out in this project can help to design new types of protection that can defend against more threats, saving time and money discarding configurations that do not work, and pointing out the configurations that seem to work better.

With the help of numerical simulations it can also be studied why some configurations work better against a certain type of threat varying parameters of the study.

1.2 Objectives

The objective of this investigation is to understand the design of ballistic materials and to study the physics behind the behavior of a specific material, Ultra High Molecular Weight Polyethylene (UHWMPE), upon impact.

This objective is too ambitious for the scope of this project, so this will be the first step in the development of the numerical simulations needed for a doctoral thesis. This project is part of an investigation project in which the Departament of Continuum Mechanics and Structural Analysis and the Deparment of Mechanical Engineering participates.

In order to understand it, it is intended to reproduce the test results obtained by M. Yong, L. Iannucci, B.G. Falzon[3] and Xiaogang Chen, Yi Zhou and Garry Wells[4].

In their experiments, Xiaogang Chen, Yi Zhou and Garry Wells test the characteristics of a plate formed by UniDirectional UHWMPE and woven UHWMPE in several configurations. After checking the viability of each material alone, a stacked plate mixing both was investigated, reaching the optimized UHWMPE plate for absorption energy.

The investigation of M. Yong, L. Iannucci, B.G. Falzon centered in obtaining a minimum weight-cost design with the highest energy absorption. They did so comparing the ballistic limit of several materials and then trying several multilayer configurations.

In our case, the material orientation and a configuration mixing UHWMPE and other materials won't be covered. Instead, a number of parameters (material characteristics and plate conditions) will be changed.

1.3 Project description

The project is divided in 8 points according to the information presented.

The first point introduces the project, the motivation to investigate it and the basis to study it. It also contains the objectives expected from this project and a brief summary of its contents.

The second point presents the background of the study, in which the evolution of personal protections is introduced, as well as previous projects and investigations. It also includes an introduction to Finite Element Methods and the program used for its analysis, ABAQUS[11].

The third point studies the socioeconomic environment, which considers the economic impact that this project might implicate and the budget needed to carry it out.

The fourth point involves the regulatory framework which includes an analysis of the existing law regarding the studied subject and a review of a NIJ standard.

The fifth point explains the state of the art, showing the experimental tests in which this study is based, presenting its results and methods.

The sixth point introduces the finite element model created for the project.

The seventh point contains the parametric study, in which several model characteristics are changed to study the reaction after impact, and collects its results.

The eighth point is dedicated to the conclusions and future works. The results obtained are compared and explained as well as the proposition of future possible projects that can be developed using the results obtained in this project.

1.4 Time Planning

In this section, a rough estimate of the hours dedicated to each task will be presented. The tasks defined for this project were:

- Definition of the problem to be solved. Tutoring hours to decide which parameters to study and what kind of model to create.
- Research time. Time used to understand the topic at hand and for the recompilation of the information needed to develop the project.
- Simulation. Time needed to create the model, generate the different cases and to run the simulations.
- Writing of the thesis using the results obtained from the simulations.

The total time is summed up in Table **??**

Task	**Hours**
Definition	6
Research	200
Simulation	952
Writing	80
Total	**1,238**

Table 1: Estimated time to complete the project

2 Background

2.1 Historical development of body armor[1]

The development of armor and weapons began with humanity itself. At the beginning, body armor and protective items, such as shields and helmets, where made from animal skin and bones. When civilizations developed, so did the materials used for defense, first with wood and later with metals. As soon as iron could start to be worked with, its used spread, as it offered more resistance than the rest of alloys used up until that moment, like bronze.

Figure 2: Evolution of armor through time.

As it can be seen in Fig. 2 the more advanced armors evolved with the technology of the era.

In the Eastern regions laminated armor was the norm. It consisted in plates of hardened skin riveted to a linen clothing, the Chinese used rhinoceros and the Mongols, ox.

The Greeks used a linen laminate known as linothorax, covered by a breastplate with helmet and greaves for protection, all made of bronze.

The Celts created the chainmail about 500 BC, which consisted in a shirt made of interlocking iron rings. Mail offered flexibility and resistance to slashing attacks, although thrusting attacks could rip through the rings, rendering it mostly useless.

Romans adopted the use of mail on their armors, although they also used scaled armor, which consisted in small iron or bronze scales sewn into a linen backing, and a type of armor called "lorica segmentata", consisting in hoops of iron fastened to leather straps.

Chainmail became the main defense up to the 14^{th} century, as it offered a high level of defense and almost no maintenance (due to the constant friction between rings, no rust was formed).

In the earlier 1300s, small plates started to be added to the chainmail suit to offer protection against thrusting threats, such as arrows or rapiers. As the plating technology advanced, mail started to be used only in areas that could not be plated, such as knees and elbows.

In 1400, a complete covering thanks to articulated plating was achieved, finally completing a full body plate armor. During this period, advances in metallurgy were made, allowing the creation of more resistant steels thanks to tempering and quenching techniques.

In 1500, the appearance of the first firearms created the necessity of the armor to be thicker to stop the projectiles, which increased its weight and reduced the stamina and comfort of the soldier wearing it.

With the increase in power and range of firearms, it became cheaper to lightly armor soldiers and arm them with fire weapons. In 18^{th} plate armors grew so heavy that were largely abandoned in favor of maneuverability and stamina for infantry, while only cavalry were heavily armored.

The creation in 1700 of the bayonet[12] marked the end of the use of body armor and helmets designed to defend against swords and pikes. This initiated a period in which armies were fitted to engage in long marches, thus equipping light armor and fire arms.

This trend continued until soldiers suffered more injuries due to explosives and projectiles, when armies started to be outfitted with body armor to avoid casualties caused by heavy artillery and explosives. Here begins the development of bulletproof vests.

2.2 Bulletproof vests[2]

With the expansion and increase in power of firearms and explosives, bulletproof vests had to evolve and become more resistant not only to different calibers, but also to different types of projectiles.

2.2.1 History

The first bulletproof vests originate in the XVI century, when a need to defend against fire arms started to arise. Those vest were based on the designs from medieval Japan, where the first types of soft armor made from silk appeared.

In the XVII century the cuirasess where made musket-proof by using three layers, the outer layers absorbed the energy of the impact and the inner one, which was thicker, stopped the bullet.
During the industrial era, in Korea, a soft bulletproof vest made of layers of cotton fabric was created to defend against the threat of Western invading armies.

Along this period, bulletproof vests were made from thick, sturdy plates of steel, which offered high resistance against shotguns and pistol bullets. While soft vests were mainly designed with multiple layers of silk.

At the start of World War I, no body armor was issued for the soldiers, but in 1915 the first protections were made, to offer some security to pilots against anti-aircraft bullets and shrapnel. The first models were made of interwoven layers of silk and cotton hardened with resin. But most of the trials to create body armor for infantry was too heavy to be used comfortably, relegating its use to static units. The soft vests kept on developing, and they started to be filled with cotton padding and cloth. This was enough to cope with the fire power of the epoch.

During World War II, Medical Divisions stated that most of the injuries being suffered could be prevented by wearing some type of light armor. This led to the development of flack jackets for the aircraft personnel. These jackets, made of nylon, could protect against flak and shrapnel, but it was ineffective against bullets.

As for infantry, most models of body armor were still to mobility limiting to be used in the open. This changed in 1944, when the Doron Plate, a fiberglass laminate, was created. This plates where inserted in nylon vests, further increasing its ballistic properties. Another body armor that had some exit consisted of two pressed

steel plates, 2mm thick, that protected torso and groin.

After the war, vests started to be made of hard materials, such as reinforced plastic or ceramic plates, woven into a nylon vest. These were the first vests capable of stopping rifle fire.

In the 70's, Kevlar was invented. A synthetic fiber, woven into fabric and layered. This material had five times the tensile strength of steel but a fraction of its weight. This material was rapidly investigated and formed the core of ballistic vests, adding several configurations like steel plates covering vital organs which reduced the blunt trauma caused by impact.

In recent years, Kevlar was found to have some flaws. If a large fragment hit the vest at high velocity, the sheer force of the impact could be fatal due to blunt trauma injuries. To overcome this problem, ceramic plates were added to the vest, to offer protection against high speed threats. This caused again that the vest were heavier and reduced mobility. Here started a period in which the objective was to find the better trade-off between protection and mobility.

The solution found was to create modular body armor, in which the vest offers protection against shrapnel and low velocity projectiles, and ceramic inserts offer protection against high velocity ones.

Since 1970, new fibers are appearing to compete with Kevlar, like Dyneema, Spectra or Twaron. But, even though they are lighter and stronger than Kevlar, they are still too expensive.

2.2.2 Performance standards

Standards are defined in each region. Around the world the type of ammo varies and as a result the armor testing must reflect the threats found locally.

One standard widely accepted is the NIJ standard, see table 2. Personal body armor covered by this standard is classified into five types (IIA, II, IIIA, III, IV) by level of ballistic performance. In addition, a special test class is defined to allow armor to be validated against threats that may not be covered by the five standard classes.

The classification of an armor panel that provides two or more levels of NIJ ballistic protection at different locations on the panel is that of the minimum ballistic protection provided at the panel.

The higher levels of protection also offer protection against threats of a lower level.

2.2.3 Investigation

To keep on developing bulletproof materials, a series of investigations are being carried out:

- **Development of new fibers.** In recent years, synthetic fibers are being investigated and developed. These fibers have higher strength and resistance, but are not suit for vesting, as ones degrade quickly or do not offer enough tenacity to stop projectiles.
- **Textile woven and laminates research.** Fabrics with finer yarns have been offering good results in ballistic prowess, but yarn size has a limit, and once that limit is reached, a new breakthrough will be needed. For now, composites interlocking steel plates and UHMWPE plates are offering good results.
- **Developments in ceramic armor.** Ceramic materials are hard to manufacture into big, torso-sized plates for the vest and this plates are prone to cracking while in use. To overcome this, it is being investigated the use of small ceramic components. These new designs can be rigid, semi-flexible or flexible and offer multi-hit performance, because if the shot is not on the exact same plate, it will still stop the bullet, contrary to bigger plates that would crack after being shot once, rendering them useless.
- **Nanomaterials in ballistics.** Currently, two methods to use nanomaterials into body armor are being researched.

  One is based on nanoparticles that become rigid when the kinetic energy threshold of the material is surpassed.

Armor Level	Protection against
Type IIA	-New armor: • 9 mm Full Metal Jacketed Round Nose (FMJ RN) bullets with a specified mass of 8.0 g (124 gr) and a velocity of 373 m/s ±9.1 m/s • .40 S&W Full Metal Jacketed (FMJ) bullets with a specified mass of 11.7 g (180 gr) and a velocity of 352 m/s ± 9.1 m/s . -Conditioned: • 9 mm FMJ RN bullets with a specified mass of 8.0 g (124 gr) and a velocity of 355 m/s ± 9.1 m/s • .40 S&W FMJ bullets with a specified mass of 11.7 g (180 gr) and a velocity of 325 m/s ±9.1 m/s.
Type II	-New armor: •9 mm FMJ RN bullets with a specified mass of 8.0 g (124 gr) and a velocity of 398 m/s ± 9.1 m/s • .357 Magnum Jacketed Soft Point (JSP) bullets with a specified mass of 10.2 g (158 gr) and a velocity of 436 m/s ± 9.1 m/s . -Conditioned: • 9 mm FMJ RN bullets with a specified mass of 8.0 g (124 gr) and a velocity of 379 m/s ±9.1 m/s • .357 Magnum JSP bullets with a specified mass of 10.2 g (158 gr) and a velocity of 408 m/s ±9.1m/s.
Type IIIA	-New armor: • .357 SIG FMJ Flat Nose(FN) bullets with a specified mass of 8.1 g (125 gr) and a velocity of 448 m/s ± 9.1 m/s • .44 Magnum Semi Jacketed Hollow Point (SJHP) bullets with a specified mass of 15.6 g (240 gr) and a velocity of 436 m/s ± 9.1 m/s . -Conditioned: • .357 SIG FMJ FN bullets with a specified mass of 8.1 g (125 gr) and a velocity of 430 m/s ± 9.1 m/s • .44 Magnum SJHP bullets with a specified mass of 15.6 g (240 gr) and a velocity of 408 m/s ± 9.1 m/s.
Type III	-Hard armor or plate inserts: • Shall be tested in a conditioned state with 7.62 mm FMJ, steel jacketed bullets (U.S. Military designation M80) with a specified mass of 9.6 g (147gr) and a velocity of 847 m/s ± 9.1 m/s. -Flexible armor: • Shall be tested in both the “as new” state and the conditioned state with 7.62 mm FMJ, steel jacketed bullets (U.S. Military designation M80) with a specified mass of 9.6 g (147 gr) and a velocity of 847 m/s ±9.1 m/s.
Type IV	-Hard armor or plate inserts: • Shall be tested in a conditioned state with .30 caliber armor piercing (AP) bullets (U.S. Military designation M2 AP) with a specified mass of 10.8 g(166 gr) and a velocity of 878 m/s ± 9.1 m/s. -Flexible armor: • Shall be tested in both the “as new” state and the conditioned state with .30 caliber AP bullets (U.S. Military designation M2 AP) with a specified mass of 10.8 g(166 gr) and a velocity of 878 m/s ± 9.1 m/s.
Special type	A purchaser having a special requirement for a level of protection other than one of the above standard types and threat levels should specify the exact test round(s) and reference measurement velocities to be used and indicate that this standard shall govern all other aspects.

Table 2: NIJ Standard-0101.06.[6]

The other is a nanocomposite reportedly able to withstand shocks of projectiles at 1.5 km/s and shock pressures of 24.5 GPa.

- **Graphene composite.** Graphene, manufactured from carbon, is the strongest and most conductive material on the planet. It tensile strength is 200 times that of steel and it dissipates energy 10 better. This makes it an interesting material to study. It is being investigated as a composite with a mixture of other materials
- **Liquid armor.** This material consists of Kevlar that is soaked into two possible fluids, a shear thickening fluid or a magnetorheological fluid. The shear thickening fluid behaves like a liquid until it suffers some kind of shear stress and it starts behaving like a solid. The magnetorheological is an oil filled with small iron particles that will line and thicken the oil dramatically when faced with a magnetic field.

2.3 Finite Element Method

The Finite Element Method (FEM) is a technique used to perform Finite Element Analysis (FEA) to obtain approximate solutions to problems encountered in any engineering analysis. In recent years, it has gained importance as FEM can divide complex problems into an array of simpler ones, easing the acquisition of information. Even though FEM has made the resolution of problems easier, it comes with a set of disadvantages:

- A general closed-form solution, which would permit one to examine system response to changes in various parameters, is not produced.
- FEM has inherent computational errors.
- Mistakes made by the user will cause incoherent or incorrect results.
- FEM only obtains approximate solutions.

FEA is a computational tool to find approximate solutions to differential equations. FEA works under the principle of mesh discretization. The model under consideration is decomposed into a set of elements called finite elements,see fig.4, creating thus a mesh that has to verify the following restrictions: the elements cannot leave any zone of the model and cannot overlap. In the same way a circle can be infinitely approximated to a set of straight lines, FEA connects the equations calculated in the elements into a more complex equation valid for the larger model.

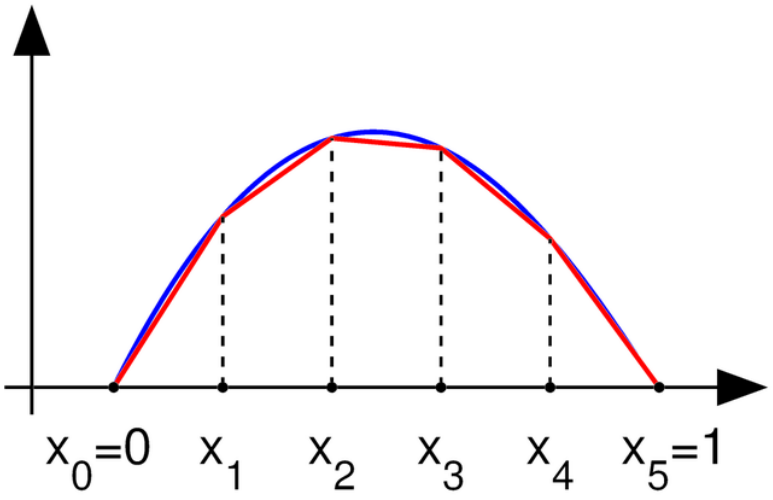

Figure 3: Approximation of a curve by division of the domain.

The more divisions done to the model, the better the accuracy of the results. But it has to be taken into account that the more elements on a simulation, the higher the computational price.

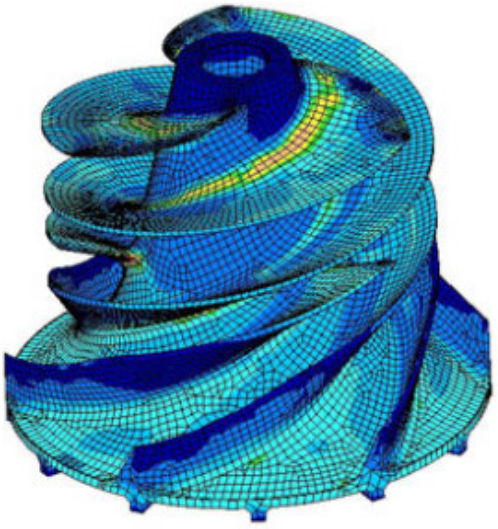

Figure 4: Complex model meshed into simpler elements.

Dividing the whole model domain into several smaller, simpler elements has several advantages[13]:

- Accurate representation of complex geometry
- Inclusion of dissimilar material properties
- Easy representation of the total solution
- Capture of local effects.

A basic usage of the finite element method includes:

1) The division of the domain into several subdomains.
2) Recombination of the sets of element equations into a global system of equations.

In the domain division, the element equations are simple equations used to approximate the original complex problem to be studied. The original equations are usually partial differential equations (PDE) approximated locally with:

- A set of algebraic equations for steady state problems.

- A set of ordinary differential equations for transient problems.

These equation sets are the element equations. They are linear if the PDE is linear, and vice versa. Algebraic equation sets that arise in the steady state problems are solved using numerical linear algebra methods, while ordinary differential equation sets that arise in the transient problems are solved by numerical integration using standard techniques such as Euler's method or the Runge-Kutta method.

In the set recombination, a global system of equations is generated from the element equations through a transformation of coordinates from the subdomains' local nodes to the domain's global nodes. This transformation includes appropriate orientation adjustments as applied in relation to the reference coordinate system. The process is often carried out by FEM software using coordinate data generated from the subdomains.

FEA simulations are such a valuable resource because they save the creation and testing of hard prototypes for experimental testing. For example, in a wing fatigue test simulation it is possible to increase prediction accuracy in the areas of interest like the union between wing and fuselage and reduce it in the tip of the wing. This would reduce the cost of the simulation.

2.4 Abaqus 6.12

Abaqus is a software used for finite element analysis and computer-aided engineering. The one used for the simulations in this project is Abaqus/CAE, or "Complete Abaqus Environment". It is an application used for both the modeling and analysis of mechanical components and assemblies (pre-processing), which are introduced into Abaqus/Standard or Abaqus/Explicit to process the data and then, visualizing the finite element analysis result in Abaqus/CAE or Abaqus/Viewer (post-processing)[14].

The FEA performed by Abaqus can be separated into three parts[15]:

1) Preprocessing:

   The user constructs a model of the part to be analyzed in which the geometry is divided into a number of discrete subregions (elements) connected at discrete points called nodes. Some of these nodes will have fixed displacements, while others will have prescribed loads.

   The creation of the model can be very time consuming to prepare, depending on the difficulty of the part to study, and commercial codes try to have the most user-friendly graphical preprocessor to assist in this first step.
   In this step, the material characteristics, the initial and boundary conditions and the applied loads have to be defined. The mesh plays a critical role in the study of the part, so an adequately sized mesh is needed. For this, a mesh sensitivity analysis has to be performed.

2) Analysis:

   The dataset prepared by the preprocessor is used as input to the finite element code, which constructs and solves a system of linear or nonlinear algebraic equations.

   Commercial codes have very large element libraries, appropriate to solve a wide range of problem types. One of FEA's principal advantages is that many problem types can be addressed with the same code, merely by specifying the appropriate element types from the library.

3) Postprocessing:

   Before graphical displays, the user would have to read through enormous amounts of numbers generated by the code, listing displacements and stresses at discrete positions within the model. With just numbers to look at, it is easy to miss important trends and hot spots, so modern codes use graphical displays to help in visualizing the results. Abaqus postprocessor displays colored contours representing the results of the analysis on the model.

   In the case of an impact analysis, the velocity of the projectile and the stresses of the plate are the most important features to observe. Once the results have been obtained, the first step can be repeated in order to improve the model to obtain better results.

Abaqus has one of the most user friendly interfaces, as it guides the user through the different steps of the FEA with its separate modules, making the navigation easier and more comprehensible[16].

2.4.1 Abaqus modules

1. **Part module**

   In this module, the "body" of the problem is created. The Part module is used to create, edit, and manage the parts in the current model. This module allows the user to:

   - Create deformable, discrete rigid, analytical rigid, or Eulerian parts. The part tools also allow you to edit and manipulate the existing parts defined in the current model.

- Create the features that define the geometry of the part, like solids, shells, wires, cuts, and rounds.
- Use the Sketcher to create, edit, and manage the two-dimensional sketches that form the profile of a part's features. These profiles can be extruded, revolved, or swept to create part geometry; or they can be used directly to form a planar or axisymmetric part.
- Assign the reference point to a rigid part.
- Create sets, partitions, and datum geometry on the part in the current viewport.

The parts can also be imported from a file containing geometry stored in a third-party format or created from a meshed part in the Mesh module.

2. **Property module**

   In the property module the tasks that can be carried out are:

   - Define materials.
   - Define beam section profiles.
   - Define sections.
   - Assign materials to sections.
   - Assign sections, orientations, normals, and tangents to parts.
   - Define composite layups.
   - Define a skin reinforcement.
   - Define inertia (point mass, rotary inertia, and heat capacitance) on a part.

3. **Assembly module**

   In the assembly module all part instances are brought together into a unique model. The individual parts can be moved in a 3D environment to fix them in the needed position to obtain the desired model.

   Once all parts are assembled they belong to a unique part if they are merged.

4. **Step module**

   You can use the Step module to perform the following tasks:

   - Create analysis steps. Within the model one or more analysis steps may be defined. The steps may change the time lapse, the type of analysis and allows to observe changes in the way parts of the model interact with each other during the course of the analysis.
   - Specify output requests.
   - Specify adaptive meshing.
   - Specify analysis controls.

5. **Interaction module**

   The interaction module can be used to define and manage the following objects:

   - Mechanical and thermal interactions between regions of a model or between a region of a model and its surroundings.
   - Analysis constraints between regions of a model.
   - Assembly-level wire features, connector sections, and connector section assignments to model connectors.
   - Inertia (point mass, rotary inertia, and heat capacitance) on regions of the model.
   - Cracks on regions of the mode

   Interactions are step-dependent objects, which means that when the user defines them, it must be indicated in which steps of the analysis they are active.

6. **Load module**

   The Load module allows to define and manage the following conditions:

   - Loads
   - Boundary conditions
   - Predefined fields
   - Load cases

   As the interactions, loads are also step-dependent objects.

7. **Mesh module**

   The Mesh module allows to generate meshes on parts and assemblies created in Abaqus/CAE. Various levels of automation and control are available so that a mesh that meets the needs of the analysis can be created.

   The Mesh module provides the following features:

   - Tools for prescribing mesh density at local and global levels.
   - Model coloring that indicates the meshing technique assigned to each region in the model.
   - A variety of mesh controls, such as:
     - Element shape
     - Meshing technique
     - Meshing algorithm
     - Adaptive remeshing rule
   - A tool for verifying mesh quality.
   - Tools for refining the mesh and for improving the mesh quality.
   - A tool for saving the meshed assembly or selected part instances as a mesh part.

8. **Optimization module**

   The Optimization module is used to create an optimization task that can be used to optimize the topology or shape of your model given a set of objectives and a set of restrictions. The Optimization module allows to perform the following tasks:

   - Create optimization tasks
   - Create design responses
   - Create objective functions
   - Create constraints
   - Create geometric restrictions
   - Create stop conditions

9. **Job module**

   The Job module performs the processing part of the FEA, transmitting the input file with the data of the whole model and its interactions to the processor, to initiate the analysis. It also manages analysis jobs and allows to view a basic plot of the analysis results. The Job module can also create and manage adaptivity analyses and co-executions.

10. **Visualization module**

    The Visualization module shows a graphical display of the results of the analysis. It obtains model information from the current model database or model and result information from an output database. You can control what information is placed in the output database by modifying output requests in the Step module. The data can be viewed from the model database using a contour plot or a symbol plot; the results data can be shown as an output database by producing a number of plots, selecting the variables introduced in the output request.

3 Socioeconomic environment

3.1 Socioeconomic impact

The research in new materials for personal protection could potentially save millions of dollars in medical fees. A better protection system would mean less people injured and that would translate into less people in need of medical attention.

If this type of material keeps on being developed, it could reach a point in time when all clothing will have some type of ballistic/slash resistance without being incredibly expensive. That would be incredibly advantageous from a social standpoint, as terror attacks or a simple mug could be potentially less perilous. If your everyday clothes could protect you from the shrapnel of an explosion or from a surprise attack with a knife people would be safer.

Clothes made from Dyneema would not only help prevent attacks. As it has great mechanical properties, it would also help in accidents. Like Kevlar, UHWMPE has great abrasion resistance so it would help to avoid scratches when falling down and absorb part of the impact.

Making clothes out of UHWMPE would not be cheap, so its use might not spread among the population due to its pricing. Because, even though the price of the material would drop if it became commonly used, clothes made out of it would be probably more expensive than clothes made out of cotton or nylon.

From an economic perspective, if this ballistic vests prove to be better than the ones currently in use, switching the current equipment used in the army would take time and money, but it could potentially help save money and lives in the long run.

This project in particular can save time and money in hard prototypes. Instead of fabricating the hundreds of panels needed to check the ballistic properties of the material, running the simulations will provide the data needed to make a proper study.

3.2 Budget

The approximate cost of the project is detailed in the following section. The costs that have been accounted for are:

- Hardware cost
- Software cost
- Personnel expenses

Hardware cost

In order to run the simulations, a personal computer valued in 1,800 euros was used. The estimated lifespan of a computer is around 5 years. Applying a linear depreciation rule, the monthly depreciation would be of 30 euros per month. This means that the hardware cost for the usage of the computer for four months (time required for the completion of the project) would be of 120 euros.

Also, an external storage device was needed to store the data from the simulations as my personal hard drive had not enough memory space in it. This external hard drive costs 80 euros.

Software cost

For this project two softwares were used MatLab and Abaqus.
The price for a standard commercial license of MatLab is 2,000 euros if no extra toolbox are needed. For this project, no extra toolbox were needed.

The price for a commercial use license of Abaqus is 25,000 euros.

Personnel expenses

The base annual salary for a junior engineer, according to "XVIII Convenio colectivo nacional de empresas de ingenieria y oficinas de estudios tecnicos" [17], is 17,544.44 euros. Assuming the estimated time for the completion of this project to be of 4 months (June - September), the total payment for the engineering time would be 5,848.15 euros.

This brings the total cost of the project to:

Budget	
Hardware cost	200 euros
Software cost	27,000 euros
Salary	5,848.15 euros
Total	**33,048.15 euros**

Table 3: Budget of the project.

4 Regulatory framework

The regulations regarding ballistic vests depend from country to country. In the case of USA, they even vary from state to state. These are some of the restrictions in some major areas:

- In the European Union, buying and selling ballistic vest is permitted, except for protection of level IV or more, which is considered for military use only. For protection under level IIIA, any citizen is free to own a ballistic vest.
- In the Netherlands the civilian ownership of body armor is not regulated and is sold in many venues, trying to offer protection to people working in the security industry.
- In Canada, except in some provinces such as Alberta or Manitoba, it is legal to buy and to wear body armor. In the regions with limitations it is necessary to have a license to own body armor.
- In Australia is illegal to import body armor without consent of the appropriate authorities. In some regions it is illegal to even posses body armor without authorization.
- In Italy it is mandatory to wear body armor for those individuals working in the security and private protection service.
- In the United States the general regulation is that anybody can purchase and own body armor, except convicted felons for violent crimes. There are some peculiar regulations in some states:

  -In Florida it is illegal to wear body armor during the commission of a crime.

  -In Kansas it is illegal to carry or wear a bulletproof vest during protests, parades, rallies, assemblies and demonstrations.

  -In Kentucky it is not prohibited to posses body armor, but parole will be denied to any person convicted of committing certain crimes while wearing it.

  -Massachusetts makes it a felony to wear body armor while committing a crime.

  -In New Jersey, a person can be charged separately for wearing a bullet proof vest while carrying out criminal acts. The practical effect is more jail time and fines.

  -Connecticut has the most strict regulations on body armor. These laws prohibit residents of the state of buying or selling body armor except face-to-face. Not abiding by this rule is punishable with up to six months of imprisonment, a 1,000$ fine or both. The law exempts sales to:

  1) Authorized officials of local police departments, the State Police, the Division of Criminal Justice, the Department of Correction, or the Board or Pardons or Parole;

  2) Authorized municipal or Department of Administrative Services' officials who buy body armor for the above agencies.

  3) Authorized Judicial Branch officials who buy body armor for probation officers.

  4) Members of the National Guard or armed forces.

4.1 National Institute of Justice ballistic standard

The ballistic resistance of body armor (NIJ standard-0101.06)[18] is a research effort to set minimum performance standards for specific devices, test commercially available equipment against those standards, and disseminate the standards and the test results to agencies nationally and internationally.

The classification of armor for this standard is shown in Table 2. This document gathers all the individual parts required to perform ballistic tests and defines and explains them. It also defines the size of the sample

needed to perform a test, because for a piece of equipment to be up to the standard, it has to fulfill all the requirements specified in section 4 of the document.

It even specifies the storage conditions the body armor needs to keep the qualities expected of it.

For example, the full standard of the ballistic test method is recorded in the document:

1. **Test order.** The ballistic test series may be performed in the order chosen by the manufacturer.
2. **Workmanship examination.** All armor samples shall be inspected before testing, to check for deficiencies, and after testing, to verify the construction details.
3. **Sampling.** The sample size will be decided according to the standard sampling method, also in this document.
4. **Sample Acclimation.** All armor samples received for testing shall be stored and acclimated for a minimum of 24 h at ambient conditions.
5. **Fair Hit Requirements for all Ballistic Tests.** For a shot to be considered a fair hit, it needs to fulfill certain conditions, e.g. hitting with an incidence angle not greater than $\pm$ 5º, no closer than a certain distance (specified in the document) from the edge nor from another previous shot.
6. **Backing Material preparation and sample mounting for all Ballistic Tests.** The clay in each fixture has to be in a block form, free of voids and smooth. The sample will be strapped to the clay block, in a way that the point of impact will be more or less centered, far from the edges.
7. **Perforation and Backface Signature Test (P-BFS).** All samples of armor will be subjected to P-BFS. Three recordings of BFS indentions demonstrate the armor's resistance to perforation. The shots will be marked accordingly to the type of armor being tested. New armor will be tested wet.
8. **Ballistic Limit (BL) determination test.** An appropriate number of armor samples, defined in the document, shall be subjected to BL tests. The ballistic performance of the sample will be estimated from the results. Each ballistic panel shall be tested in accordance with the procedures shown in the standard.

5 State of the Art

The material tested is Ultra High Molecular Weight Polyethylene (UHWMPE) gel spun in fibers, also known as Dyneema [19][20]. This material is being researched thanks to its high yield strength, which can be as high as 2.4 GPa, and its low density, 0.945 g/cm^3. Some high-strength steels have comparable yield strengths, but since steel has a density of 7.8 g/cm^3, this gives strength-to-weight ratios for UHWMPE in a range from 8 to 15 times higher than steel.

This project is based on three previous experiments that will be explained to understand the starting point of this investigation.

5.1 Efficient modeling and optimization of hybrid multilayered plates subject to ballistic impact[3]

The objective of this experiment was to study the ballistic behavior of several materials and the way they would work as a hybrid system to obtain the minimum weight/cost design to stop bullets. As most of the experiment is beyond the scope of this project, the part concerning Dyneema will be the one summarized.

The initial test was performed on a plate of 50x50 mm of approximately 2 mm in thickness[3]. The plate was fully clamped and the different plies of the specimen were not glued between them, see Fig. 6.

The test consisted on a spherical bullet of 6 mm in diameter and 0.89 g made of stainless steel being shot with a single stage gas gun towards the Dyneema plate at increasing velocities. The objective of the test was to ascertain the energy absorption of the material and the protection it can offer against this kind of threat.

As the projectile is relatively smaller than the yarns of Dyneema, a woven fabric is more prone to projectile slip-through,see Fig.5, thus a UniDirectional (UD) fabric is used.

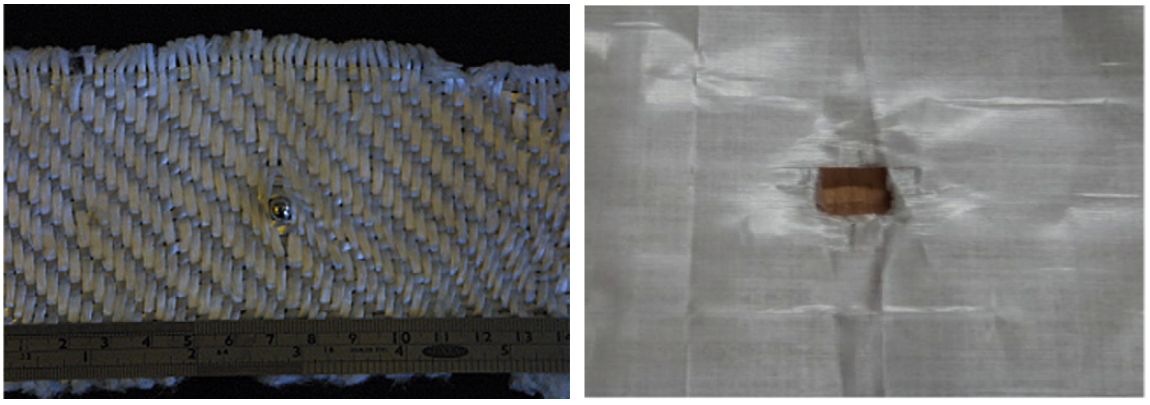

Figure 5: Projectile slip-through through the woven fabric and perforated UD specimen.

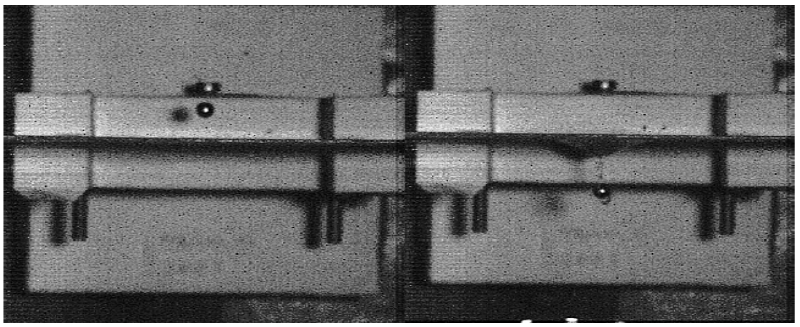

Figure 6: Test arrangement.

The experimental test was properly validated with a Finite Element (FE) model, consisting in two through-thickness elements which were found to be adequate in modelling the response of the material, with a 25x25 mesh being used to model the 50x50 mm plate[3].

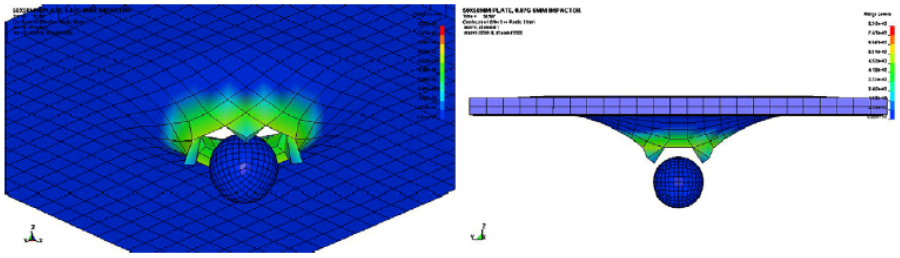

Figure 7: FE model.

After the firing test and the simulation, the following ballistic curve was obtained:

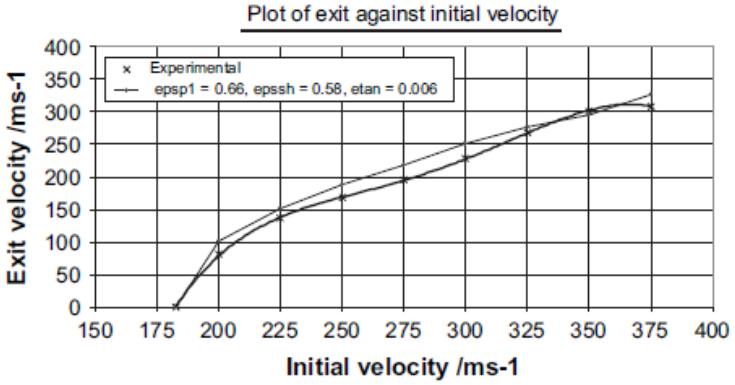

Figure 8: Ballistic curve of UHMWPE.

5.2 Numerical and experimental investigations into ballistic performance of hybrid fabric panels[4]

This paper studies the characteristics of Dyneema as a woven material and as a unidirectional (UD) material and investigates their ballistics properties. The ultimate objective is to obtain a hybrid panel with the best behavior possible against bullets.

In order to do this, both penetration and non-penetration tests were carried out on the material. The results were compared with those of a FE model.

5.2.1 Model description

The projectile for the model represents the exact same projectile used in the experimental setup. It is a projectile of cylindrical shape with diameter and height of 5.5 mm, and a mass of 1 g.

For the model of the woven fabric a yarn density of 6.73 threads per cm and an areal density of 240 g/m^2 is used. The model is 10 cm by 10 cm and is impacted at 500 m/s, which is the highest velocity measured in the experiment. The friction coefficient between yarns is 0.14, and between projectile and fabric it is 0.175.

The yarn mechanical properties are shown in Table 4:

E_{11}	E_{22}	E_{33}	G_{12}	G_{13}	G_{23}	ν_{12}	ν_{13}	ν_{23}
130	1.21	1.21	3.28	3.28	0.504	0.2	0.2	0.2

Table 4: Material parameters (GPa) for UHMWPE yarn.

As for the UD fabric, it is simulated with 3D solid continuous elements. The fabric is partitioned into four layers to simulate different fiber orientations in the fabric. The bulk density of the UD fabric is 0.8 g/cm^3 with a thickness of 0.18 mm. Other material characteristics are similar to those of the woven fabric.

The results of the models were validated with experimental results from previous works:

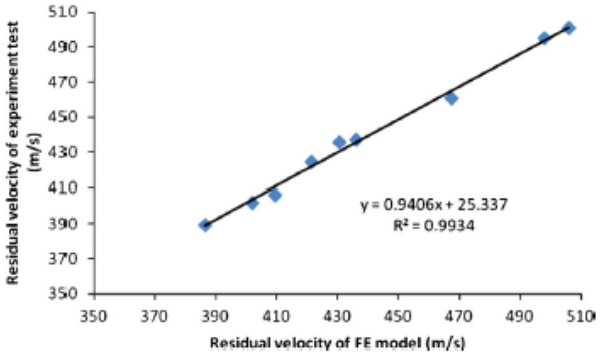

Figure 9: Comparison of FE and experimental residual velocities for the woven fabric.

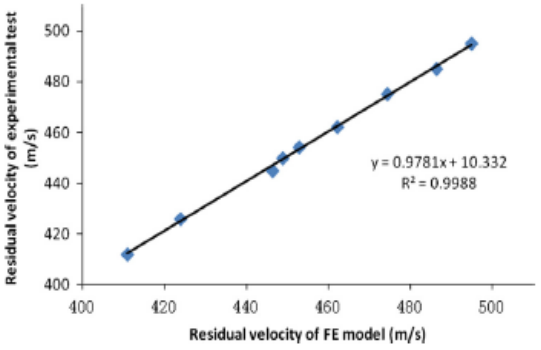

Figure 10: Comparison of FE and experimental residual velocities for the UD fabric.

The gradient of the regression line in Figs. 9 and 10 shows a good agreement between the FE models and real fabrics.

Once the models were validated a twelve-layered model was built to investigate the response of different layers upon impact on a panel.

From the results of the simulation the conclusion that the front layers mode of failure is due to shear stress and the back layers fail due to tensile stress can be drawn, as observed in Fig.11

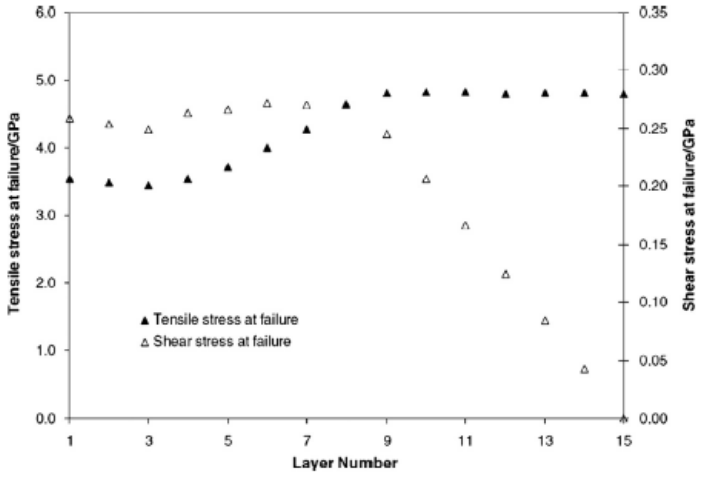

Figure 11: Predicted tensile and shear stress at the moment of failure for different layers.

5.2.2 Experimental setup

The projectile, as explained before, is a 1 g, cylindrical projectile with length and diameter of 5.5 mm. The projectile is propelled by a powder cartridge, giving a velocity in the range from 400 to 500 m/s.

For the penetration test, a single layer fabric sample is fixed on a clamp with an aperture diameter of 15cm. The performance of the sample is measured by the kinetic energy loss of the projectile, measured by:

$$\Delta E = \frac{1}{2} m(v_1^2 - v_2^2) \tag{1}$$

where ΔE is the energy loss of the projectile, m is the mass and v_1 and v_2 are the impact velocity and the residual velocity respectively.

As for the non-penetration test, a panel made of sufficient layers to stop the projectile is mounted unclamped against a clay block in which the back face deformation will be printed. As the panel won't be perforated, the ballistic performance is measured by the amount of layers fractured and the depth of the back face signature. The results for the penetration test are shown in Fig.12:

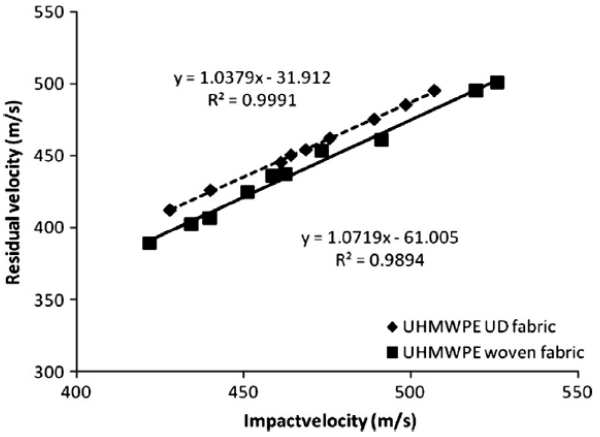

Figure 12: Ballistic protection of single-layer UHMWPE woven and UD fabrics.

The energy absorption of woven and UD fabric assemblies was also tested. Due to the limitation of the

clamp, the maximum number of fabric layers that could be fixed was 8 layers of woven fabric and 13 layers of UD fabric.

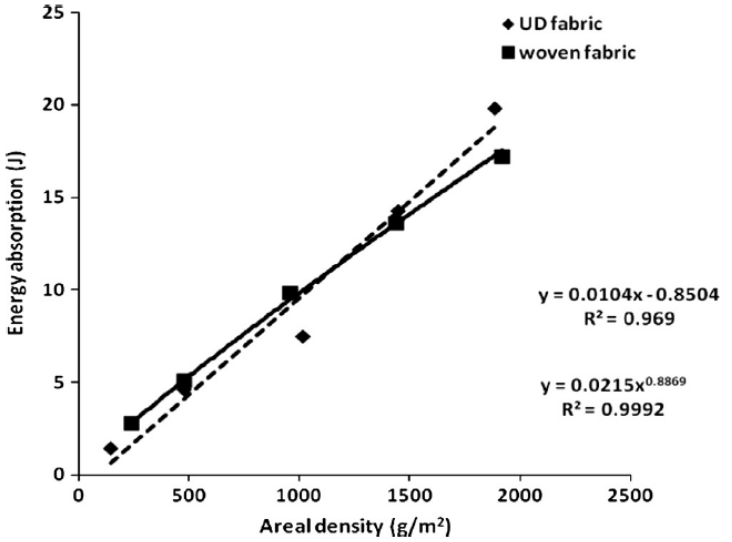

Figure 13: Comparison of energy absorption between woven and UD fabric assemblies.

In Fig. 13 can be observed that, at low areal density, the woven fabric absorbs more energy up to 1200 g/m^2, when UD assemblies absorb more energy.

Thus, for the case of the 8 layered woven assembly and the 13 layered UD assembly, with an approximate areal density of 1900 g/m^2, it is found that the UD assembly shows a higher ballistic performance (absorbing 17.4 J) than the woven assembly (absorbing 16.5 J).

5.3 Statistical dynamic tensile strength of UHMWPE-fibers[5]

The objective of this investigation was to study if temperature and strain rate had any impact on the mechanical properties of UHMWPE fiber bundles. This will be done by using the dynamic fiber-bundle testing method, because there is not an experimental technique available to perform the dynamic single-fiber tests, due to its high technical difficulty.

"The test was performed on a bar-bar tensile impact apparatus. Through the impact of a hammer on the test block, the prefixed short metal bar which is connected to the block and the input bar deforms and breaks. So an incident stress impulse is produced. Such stress impulse travels down the input bar and is partially reflected at the input bar/specimen interface and partially transmitted to the specimen and the output bar. The history of the incident strain $\epsilon_i(t)$; reflected strain $\epsilon_r(t)$ and transmitted strain $\epsilon_t(t)$ are recorded at strain gages mounted on the input bar and output bars, respectively.

The rise time and amplitude of the incident stress wave are determined by the impact velocity and the diameter of the prefixed short metal bar. So by varying the impact velocity and the diameter of the prefixed short metal bar, the tensile impact tests for any strain rate can be performed. The temperature chamber is placed between the input bar and output bar, which can be used to achieve the environmental temperature up to 120 ^oC."

The test was conducted at two high strain rates (300/s and 700/s) and at two temperatures (25 °C and 70 °C). The following figure 14 shows the stress-strain curves for each condition.

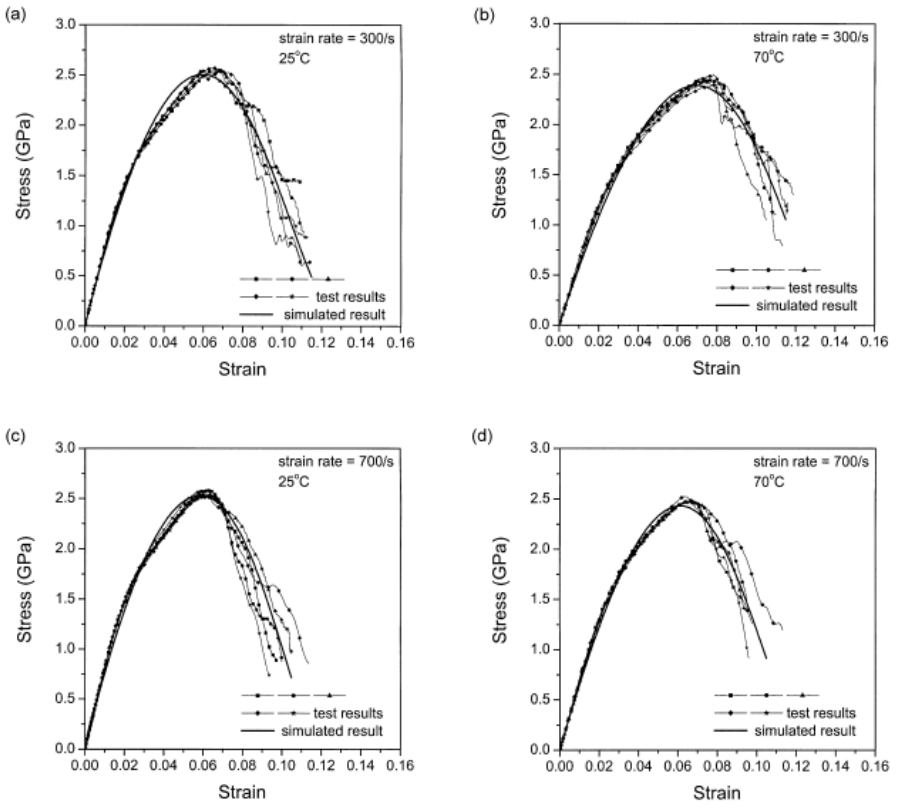

Figure 14: Stress–strain curves of UHMWPE fiber bundles at different strain rates and temperatures.

And the mechanical properties are collected on table 5.

		$E(GPa)$	$\sigma_b(GPa)$	$\epsilon_b(\%)$
300/s	25°C	80	2.55	6.52
	70°C	61	2.47	7.54
700/s	25°C	82	2.55	6.26
	70°C	68	2.48	6.57

Table 5: Mechanical properties of UHMWPE fiber bundles.

6 Model description

The FE model used tried to reproduce the experiment as closely as possible. First the geometry of the mesh was decided, and a ply of the plate and the bullet were modeled. Following this, the material properties were added and the boundary conditions imposed.

All parameters were subjected to change as deemed necessary for the various analyses carried out on the model.

6.1 Geometry

The model consists on two different parts, the plies that will form the plate, and the projectile that will be shot.

6.1.1 Plate

For the plate, as in the experiment, a 50x50 mm square is designed. The full plate is achieved by stacking a number of plies. The ply was designed with three different zones to mesh, the closer to the point of interest (the point of impact in this case), the finer the mesh is. A balance between computational time and accuracy of the results was carried out as it will be explained in section 7.1.

The ply was designed with one thickness element of 0.19 mm.

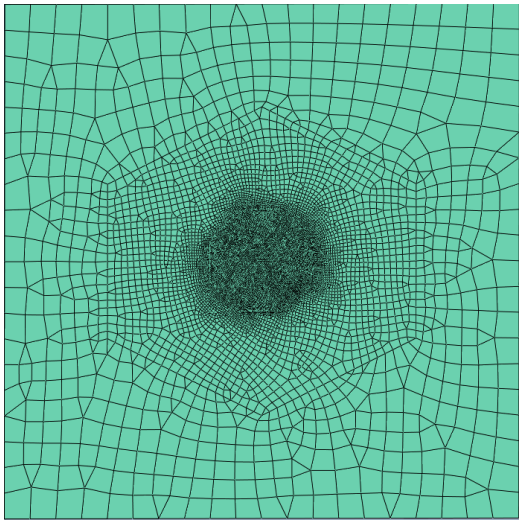

Figure 15: General mesh.

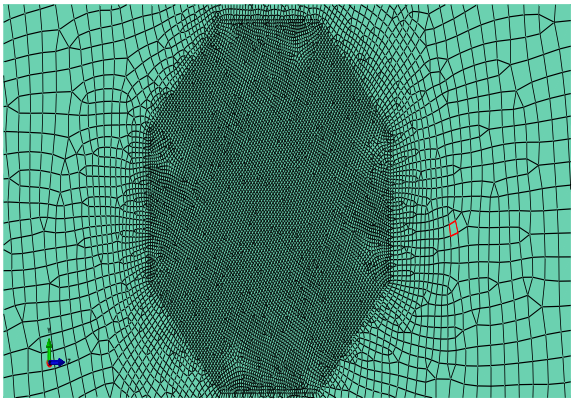

Figure 16: Mesh detail.

Excepting the study in which the number of elements of the plate is changed, the ply used is the one shown in Fig. 15. This mesh has a total number of elements of 16103, concentrating 12000 of those elements in the central part, as it can be observed in Fig. 16, and 31318 nodes.

The coordinates of the vertex of the polygonal forms inside the plate, in clockwise order, are:

Hexagon

X	Y	Z
0	15	0
0	7.5	15
0	-7.5	15
0	-15	0
0	-7.5	-15
0	7.5	-15

Octagon

X	Y	Z
0	5	2
0	2	5
0	-2	5
0	-5	2
0	-5	-2
0	-2	-5
0	2	-5
0	5	-2

Table 6: Vertex coordinates.

6.1.2 Projectile

Two different kind of projectiles were tested, a solid stainless steel ball, 6 mm in diameter and 0.89 g in weight and a 9 mm classic bullet [21].

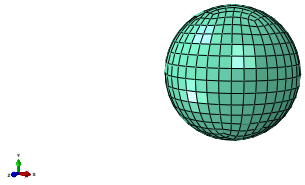

Figure 17: Spherical projectile

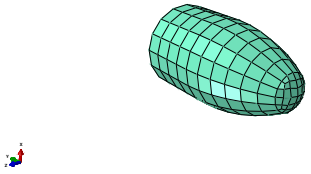

Figure 18: 9mm bullet

Both projectiles have solid elements, the sphere has 15705 elements and the bullet has 560.

6.1.3 Complete model

One complete model consist of 11 plies stacked and a projectile, leading to a total of 192.838 elements. With the number of elements being processed on each job the amount of time required for one simulation to be done was of approximately 3 hours.

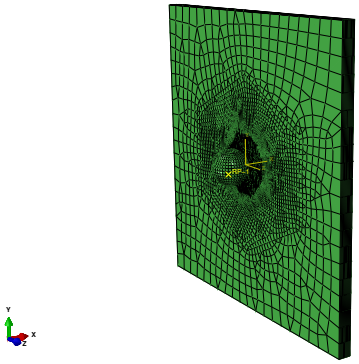

Figure 19: Assembly of the whole model.

6.2 Material properties

6.2.1 Dyneema

Composite material model considers both plastic behavior and influence of strain rate.

These properties were obtained from Ref. [4] and [5]

E (GPa)	$\rho(g/cm^3)$	ν
68	0.97	0.2

Table 7: Dyneema properties

As the problem is highly plastic, the following stress-strain curve[5] at two different strain rates were parametrized to reproduce the influence of the strain rate:

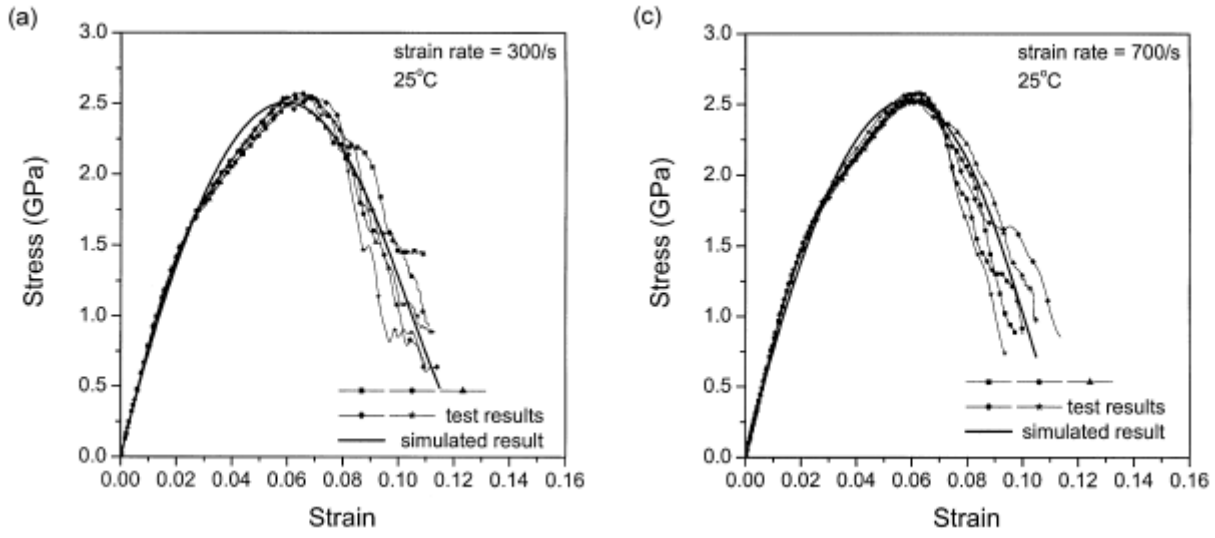

Figure 20: Stress-Strain curves

Fig. 20 shows the stress-strain curves obtained at strain rates of 300 s^{-1} and 700 s^{-1}, where the influence of strain rate can be observed. The failure stress does not change apparently with the strain rate and the maximum strain is very similar for both rates. The elastic behavior was considered strain-rate independent with a Young modulus of 68 GPa. Once yield stress was reached, the plastic behavior was determined as a function of strain rate following the corresponding stress-strain curve.

Material failure in Abaqus:

Abaqus failure treatment was not as accurate as needed for the objective of this project, so an external subroutine was used to model the failure.

This user subroutine is used to define a maximum strain criterion. This criterion allows the removal of the elements that presents strains higher than the maximum defined as a function of strain rates.

An interpolation was conducted for values of strain rate different to those obtained in experimental tests. Yield stress was also defined as a function of strain rate. For instance, yield stress was equal to 1397 MPa for a strain rate of 300 s^{-1} and equal to 1365 MPa for a strain rate of 700 s^{-1}. Thus, a linear plastic behavior considering plastic strain and strain rate dependent behavior was implemented.

Finally, an erosion criterion was included to delete damage elements considering the influence of strain rate on the ultimate strain observed in experimental tests.

The subroutine acts as an intermediary between Abaqus and a compiler.

The subroutine was built and proportionated by the UC3M departments “Department of Continuum Mechanics and Structural Analysis and the Department of Mechanical Engineering”.

6.2.2 Steel

Both projectiles are made from steel.

E (GPa)	$\rho(g/cm^3)$	ν
210	7.87	0.3

Table 8: Steel mechanical properties

As the damage properties for the plastic damage have to fulfill Johnson-Cook damage criteria, see section 6.5, the material constants are also included:

d1	d2	d3	d4	d5	A	B	C	n	m
0.05	0.8	-0.44	-0.046	0	980	2000	0	0.83	1.4

Table 9: Steel damage properties.

The data from table 9 was obtained from UC3M ”Department of Continuum Mechanics and Structural Analysis and the Department of Mechanical Engineering”.

Material failure in Abaqus:

The model applied to control the plastic failure of the steel projectile is the Johnson-Cook failure criteria, explained in 6.5.

6.3 Boundary and initial conditions

In the following figure 21 the boundary and initial conditions can be observed:

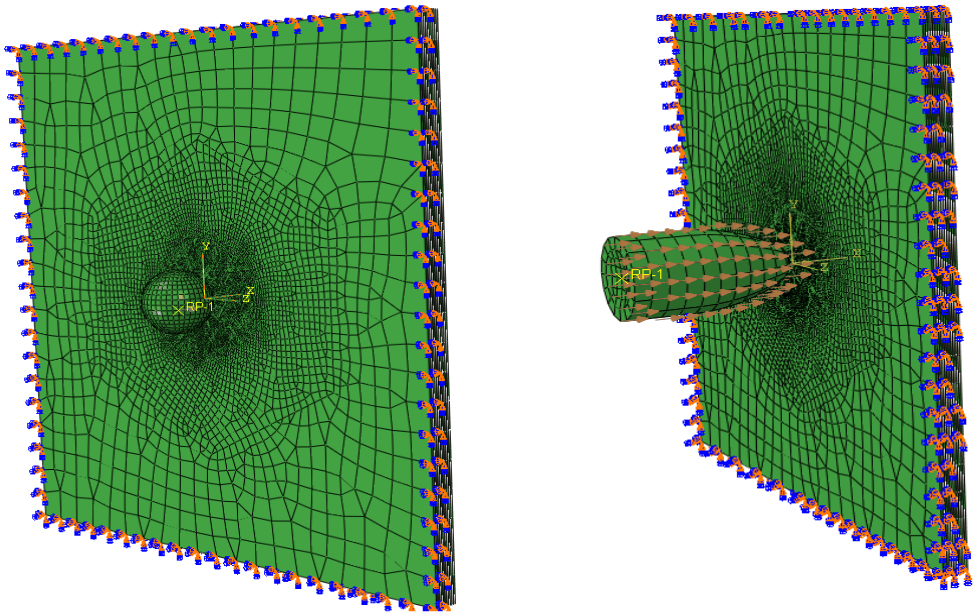

Figure 21: B.C. and I.C for the spherical projectile and for the bullet.

Interactions

A general contact between parts was defined. The properties given to this contact were:

- Normal behaviour: Hard contacts were defined so that each ply could interact with each other and amongst themselves after the bullet impact. Also separation after contact was allowed, due to the non-glued plies having free movement after impact.
- Tangential behaviour: A penalty due to friction was imposed, having a friction coefficient of 0.175.

Constraints

The Dyneema plate was clamped on its edges, so an encastre boundary condition was imposed on every border of each ply.

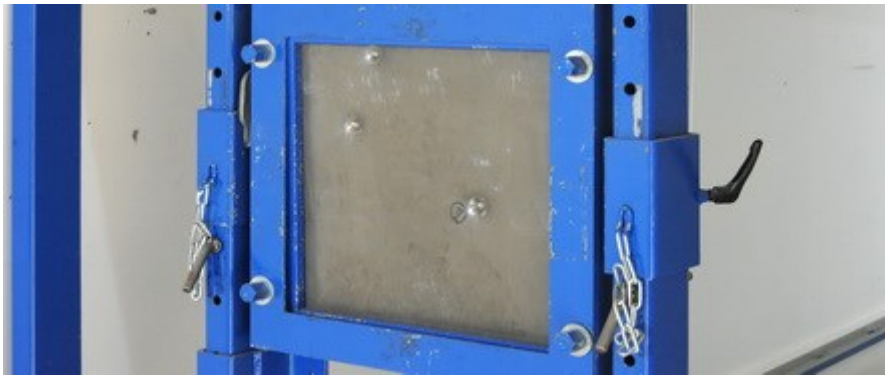

Figure 22: Boundary condition of the plate.

For the study of the behavior of a rigid solid bullet, the rigid body condition was imposed on the sphere. A control point was defined inside the body of the sphere to control the evolution of the velocity.

Initial conditions

The velocity of the projectile was simulated by imposing a velocity field of the required magnitude. For the study of the rigid body behavior, this velocity is applied at the control point, whereas for the study of the elastic and plastic behavior, the velocity is applied to every node, so that the whole body acquires the necessary velocity.

6.4 Control variables

The variables needed to compare with the experimental results are displacement, velocity, strain and stress.

- The velocity of the bullet is obtained from the control point in the body, checking it at the end of the step or after the bullet has pierced the plate completely.
- Strain and stress are checked to observe the behavior of both the projectile and the plies.
- The energy absorbed by the plate can be obtained knowing the initial and final speed.

6.5 Johnson-Cook failure model

The fracture criterion proposed by Johnson and Cook [22] considers the separated effects of strain stress-induced, strain-rate and temperature.
The constitutive equation of the model is:

$$\sigma = [A + B\varepsilon^n][1 + Cln\dot{\varepsilon}^*][1 - T^{*m}] \tag{2}$$

Where ε is the equivalent plastic strain, $\dot{\varepsilon}^* = \dot{\varepsilon}/\dot{\varepsilon}_0$ is the dimensionless plastic strain rate for $\dot{\varepsilon}_0 = 1.0\ s^{-1}$ and $T^* = \frac{T-T_{room}}{T_m-T_{room}}$. Here, T is the temperature (°C), T_{room} is the room temperature (°C) and T_m is the melting temperature of the material (°C)[23].

A, B, C, m and n are material properties determined from mechanical tests. A is the yield stress, B and n represents the effect of strain hardening, C is the strain rate constant and m is the thermal softening constant.

As the projectiles can be subjected to high strain rates, an extension of the model is needed. This model is referred to as the "Johnson-Cook dynamic failure model."

This failure model is based on the value of the equivalent plastic strain at element integration points; failure is assumed to occur when the damage parameter exceeds 1. The damage parameter, ω, is defined as

$$\omega = \sum \frac{\Delta\varepsilon^{pl}}{\varepsilon_{p,f}} \tag{3}$$

where $\Delta\varepsilon^{pl}$ is an increment of the equivalent plastic strain, $\varepsilon_{p,f}$ is the strain at failure and the summation is done at every integration point.

The dynamic failure model equation is:

$$\varepsilon_f = [D_1 + D_2 \exp(D_3\sigma^*)][1 + D_4 ln(\frac{\dot{\varepsilon}^{pl}}{\dot{\varepsilon_0}})][1 + D_5 T^*] \tag{4}$$

where D_1–D_5 are material parameters, $\sigma^* = \sigma_m/\sigma_{eq}$ is the stress triaxility ratio, σ_m is the mean stress and $\dot{\varepsilon}_0$ is the reference strain rate.

The failure model assumes that damage accumulates in the element during plastic strains which accelerates when the damage reaches a critical value.

7 Parametric study

The aim of this project is to observe the effect that changing some material parameters has on the ballistic properties of UHMWPE. To do this, a sensitivity test was carried out on the mesh, to obtain the most optimal number of elements on the mesh to obtain accurate results without overloading the computer resources.

After that, the model was validated with the results obtained from the experiments in section 5.

7.1 Number of elements of the grid

The first step was to obtain a mesh with a sufficiently large number of elements per ply as to not obtain false results, but not large enough to be incorrect due to accumulation of errors. This had to be balanced with the required simulation time for that mesh. Thus, various meshes were tried, simulating the impact at 300 m/s.

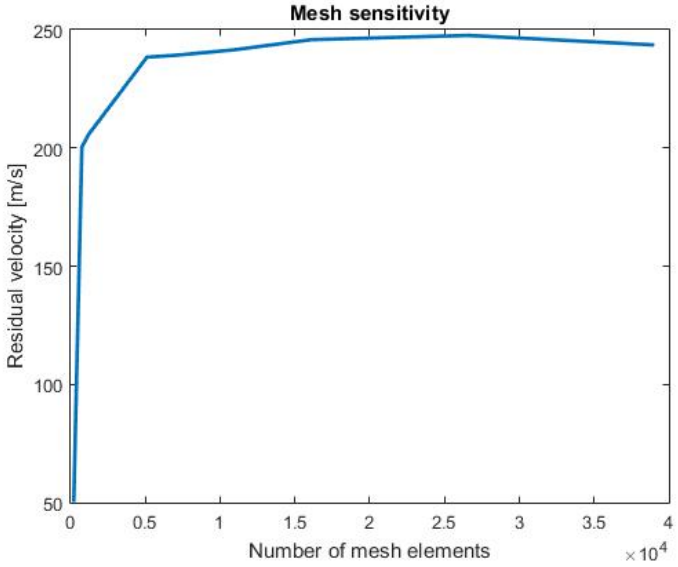

Figure 23: Residual velocity vs number of elements.

The mesh chosen, as stated before, was the one with 16103 elements because it offered the most consistent results with an acceptable resources consumption. The amount of time required for the simulations increased substantially with the addition of elements.

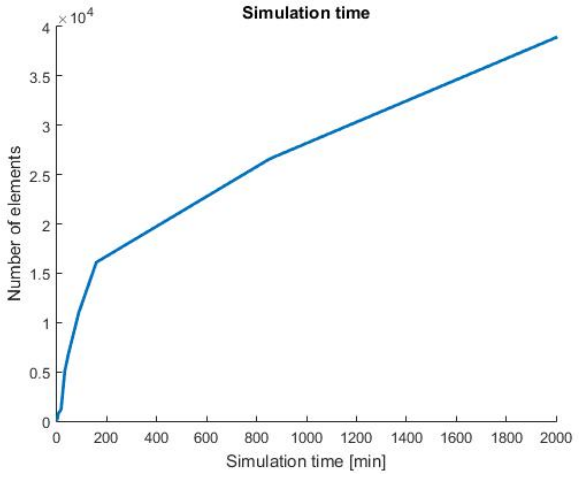

Figure 24: Evolution of simulation time with the number of elements-

The mesh selected required approximately 2h 30min per simulation

7.2 Model validation

After selecting the mesh, a model constructed with it was tested to check whether the results were accurate with respect to the experiments in which this project is based on.

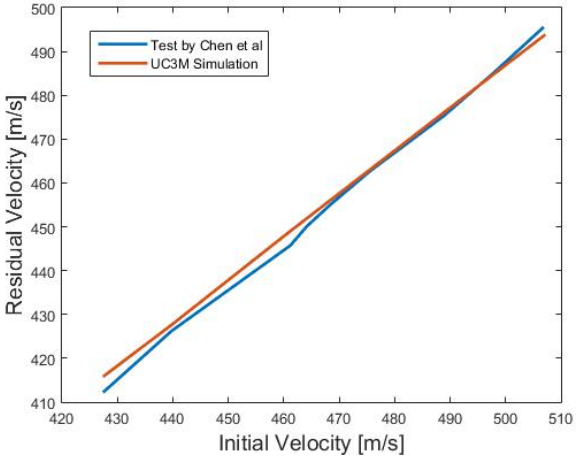

Figure 25: Validation of simulation results with Chen's experiment.

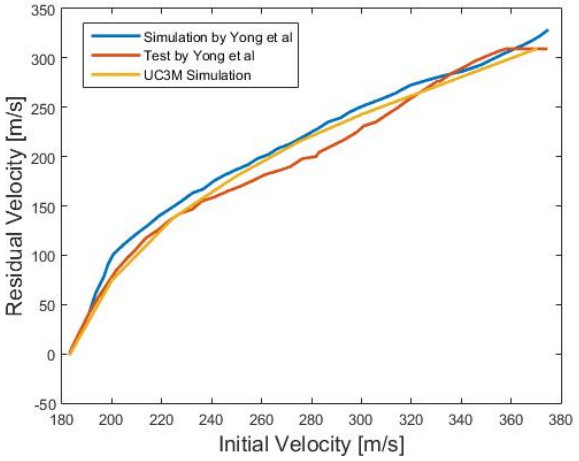

Figure 26: Validation of simulation results with Yong's experiment.

It can be observed that the model reproduces the results obtained by Chen and Yong almost identically. As the model results are validated with those of the experiments, the parametric study can be started.

7.3 Ballistic limit

The first point of interest was to find the V_{50}, or the speed at which half the bullets are completely stopped, of the model. For that, a series of simulations were run varying the initial velocity of the projectile between 100 m/s and 300 m/s.

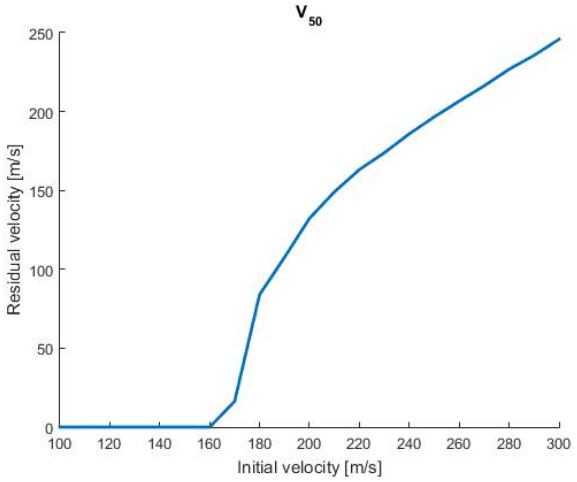

Figure 27: Ballistic limit of the model.

It was found that the ballistic limit of the model is 170 m/s, if the projectile is faster than that, the panel will not be able of stopping it.

The amount of energy absorbed by the 11 plied panel can be seen in Figs. 28 and 29.

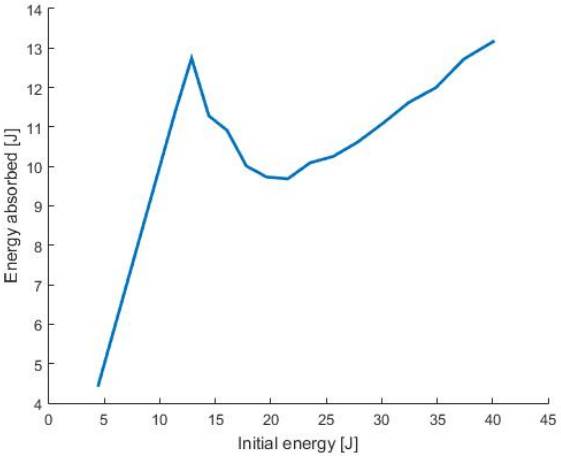

Figure 28: Energy absorbed vs Initial energy.

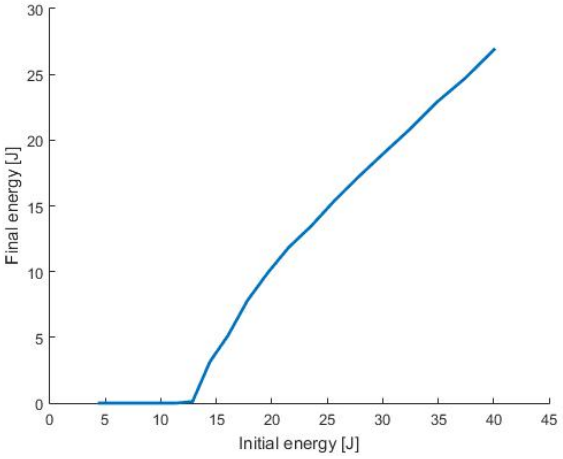

Figure 29: Final energy vs Initial energy.

It can be observed that, up until the breaking point, the panel can absorb at best 13 J of energy. After that, it absorbs less energy, as the projectile breaks through the plies without engaging all the surface. The reason why the energy peaks is because the damaged zone is big. If the velocity is increased, damage starts to concentrate only on the contact surface, creating a smoother drill. This would mean that the contact and energy transfered would be less than in the case of ripped holes.

At the velocities tested in these simulations, the plies where ripped and the damaged zone was still pretty big.

7.4 Young Modulus variation

The first parameter changed was the Young Modulus. This was done by obtaining the slope of the natural young modulus (68 GPa), and applying a correction factor for each of the proposed values (40, 52 and 80 GPa). Once the slope of each modulus is known, an extrapolation with the plastic curves of the material is done, eliminating the portion of the plastic curve that is now elastic due to the change in modulus.

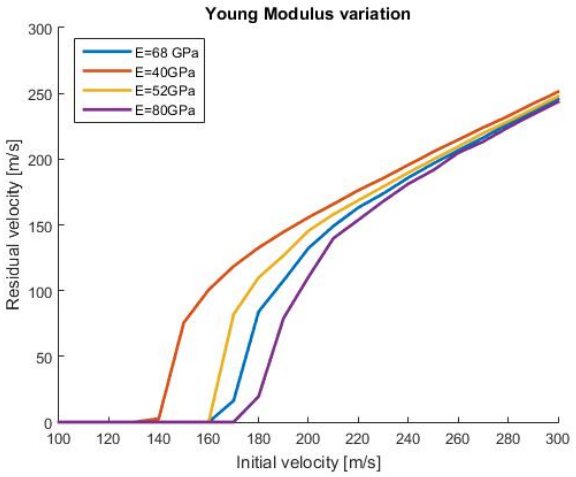

Figure 30: Varying the Young modulus.

It can be observed that the evolution of the residual velocity is more or less lineal with respect to the Young modulus. This implies that if the Young modulus of the material is higher, the absorbing ability of the vest increases.

The Young Modulus has an influence in the material at low velocities more than at hich velocities because at low velocities the plate deformation is global and is affected by rigidity, while at higher velocitites the damage becomes local.

As Chen[5] proved, UHMWPE's modulus is affected by temperature. Thus, if the vest has to perform at high temperatures (>70º C), the resulting vest will have worse results than if it were acting at colder temperatures.

The energy absorption of the different Young modulus is represented in figures 31 and 32:

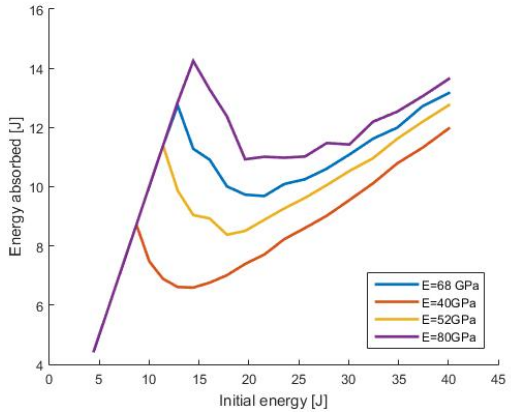

Figure 31: Energy absorbed vs Initial energy.

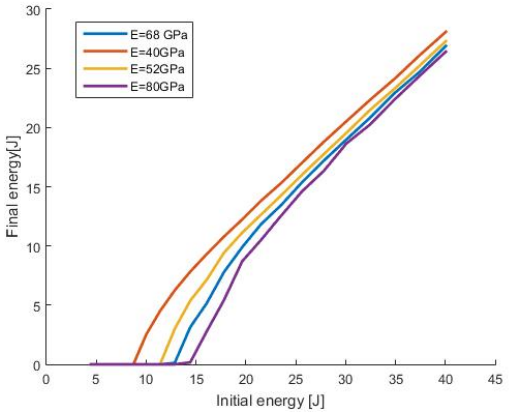

Figure 32: Final energy vs Initial energy.

As with the velocity, the energy absorption is directly related with the magnitude of the Young modulus. With a higher modulus, more energy can be absorbed before the panel breaking completely.

7.5 Strain rate variation

Afterwards, the strain rate was modified by applying a factor to the strain rates curves. The new strain rates added can be observed in Fig.33

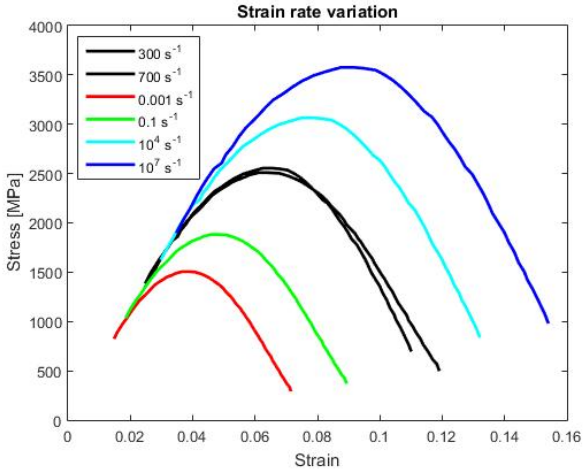

Figure 33: New strain rate curves.

These new curves were added to the material to study if they would have any effect on the response against impact.

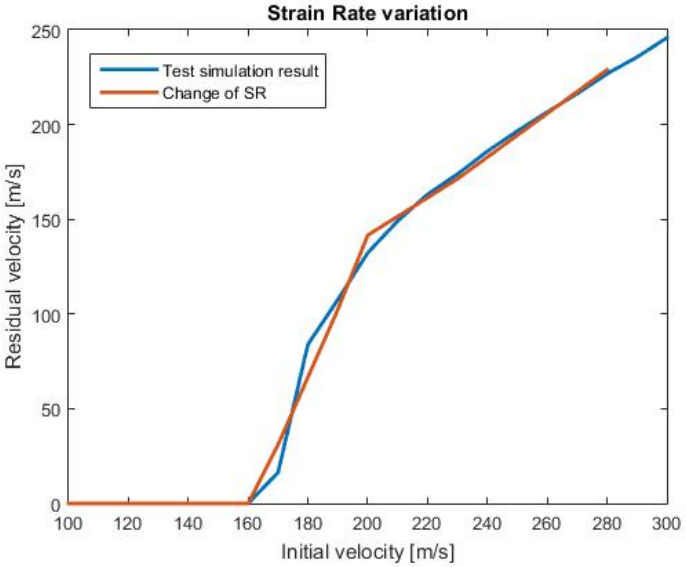

Figure 34: Varying the strain rate.

As it can be observed in fig. 34, there is not much of a change once the variation is introduced.

The energy absorption of the material after changing the strain rate is represented in figures 35 and 36:

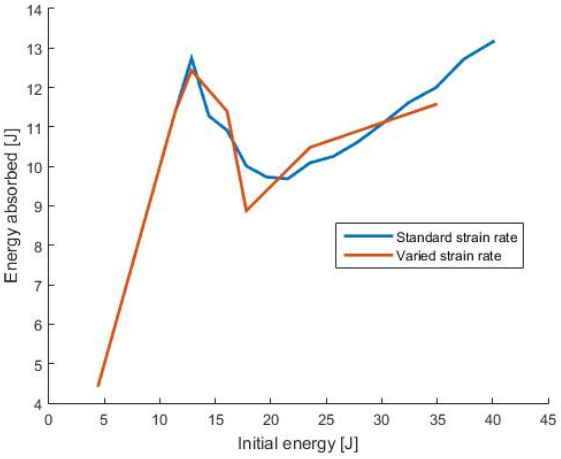

Figure 35: Energy absorbed vs Initial energy.

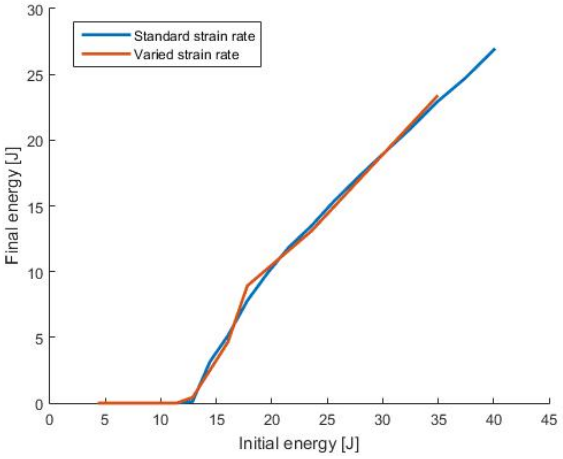

Figure 36: Final energy vs Initial energy.

In Fig. 35 can be observed how the material can absorb less energy with the new plastic curves. Even though is not much of a difference, after changing the strain rate the panel will break earlier than without the change. This could not be observed in Fig. 33.

It seems like the influence of the deformation velocity is lineal, so extrapolating between 300 s^{-1} and 700 s^{-1} the results are accurate enough.

7.6 Number of plies variation

One of the easiest ways to increase the ballistic limit of a vest is to increase its thickness, but in doing so, the weight is also increased. It is necessary to reach a point of trade off in which the vest offers the best of its

capability while not being too cumbersome.

The evolution of the residual velocity with the number of plies of the panel can be seen in Fig. 37

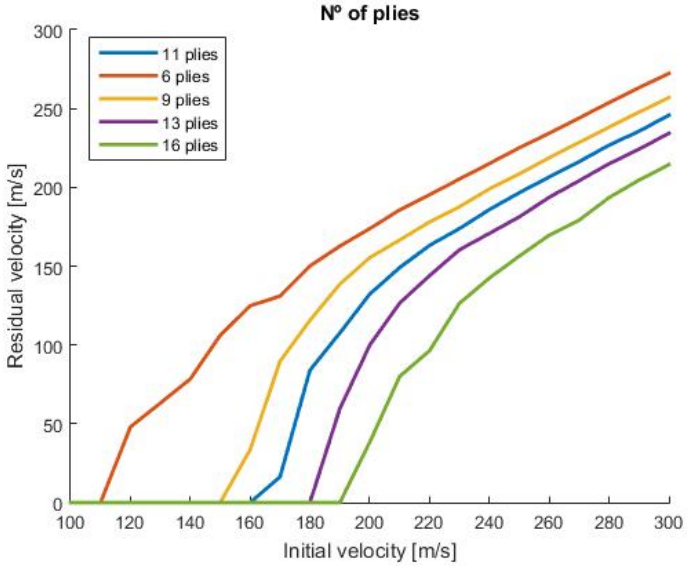

Figure 37: Varying the number of plies.

As it was expected, with the increase of the number of plies, the ballistic limit is also increased. Assuming that for more than 9 plies the increase is linear, it would mean a 10 m/s ballistic limit increase per 2-3 plies.

In figures 38 and 39 can be observed how the energy of the system evolves with the number of plies.

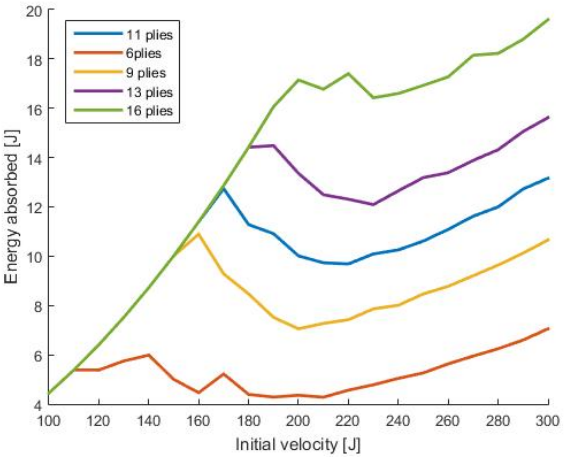

Figure 38: Energy absorbed vs Initial energy.

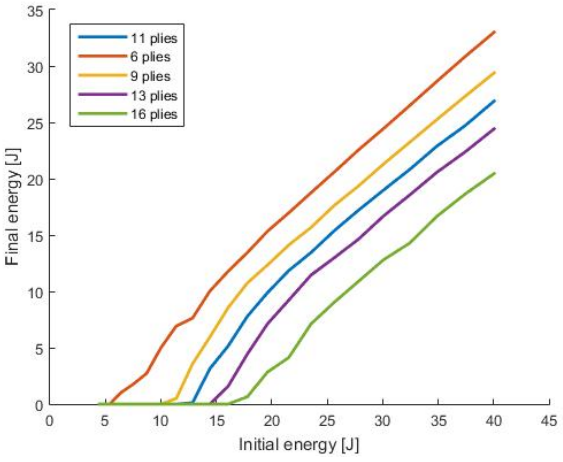

Figure 39: Final energy vs Initial energy.

7.7 Behavior of the projectile

Another parameter that could affect the simulation was the mechanical behavior of the projectile. Instead of treating it as a rigid solid, the projectile was treated as an elastic and as a plastic solid. It also was tested what would happen if instead of an sphere of 1g, a bullet shaped projectile of 6g was used.

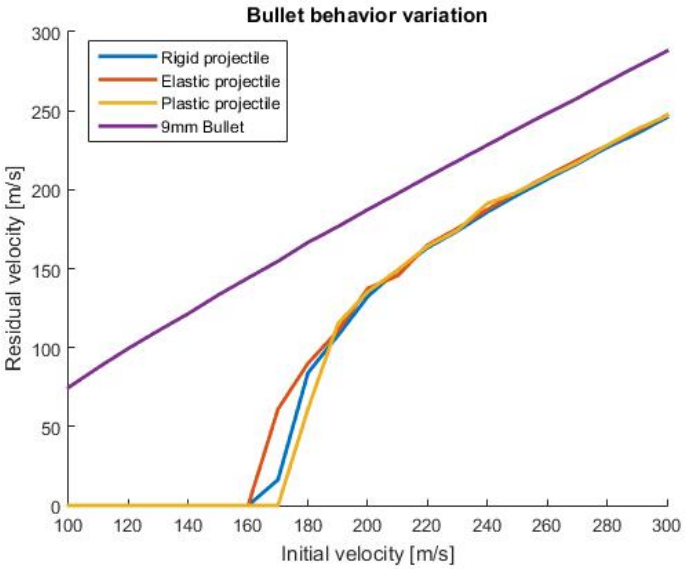

Figure 40: Varying the mechanical properties.

It can be observed that taking into account the plastic deformation of the projectile increases the ballistic limit. This might be due to the projectile changing shape and increasing the contact surface, thus distributing the energy over a larger surface, engaging more of the material.

As long as the projectile used is a sphere, it can be modeled as a rigid solid, simplifying the model and saving in computational costs because modeling it as an elastic or plastic body has not much of an effect.

As for the bullet sized projectile, the increase in mass makes a substantial difference in the amount of energy the bullet delivers, overcoming by a large margin the capacity of the plate.

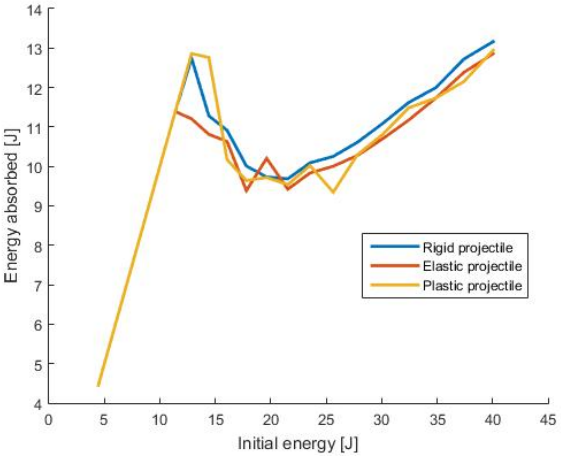

Figure 41: Energy absorbed vs Initial energy.

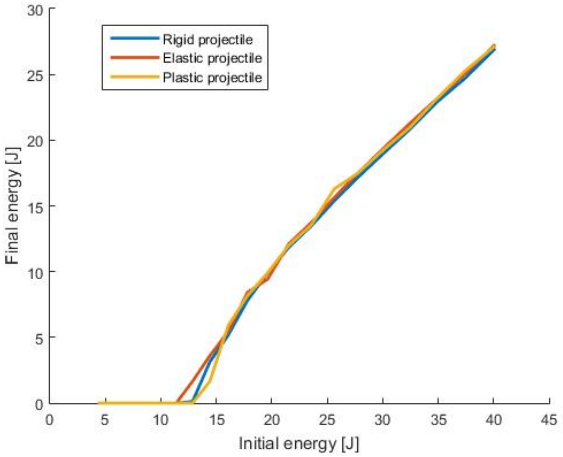

Figure 42: Final energy vs Initial energy.

It fig. 41 can be observed how the elastic projectile loses less energy and so, it breaks the panel faster.

The energy trade off of the bullet had to be represented in another graph for clearness, as the magnitude is totally different to the sphere.

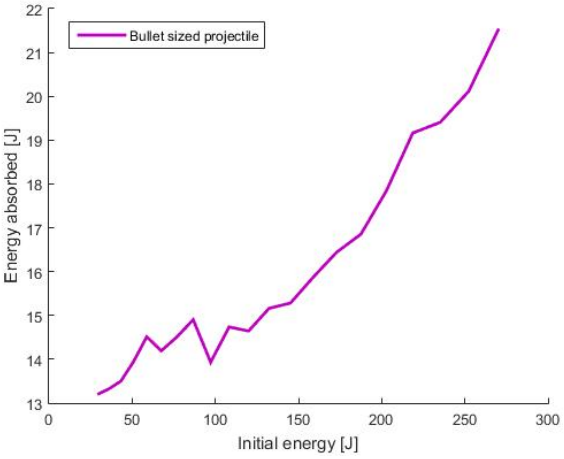

Figure 43: Energy absorbed vs Initial energy.

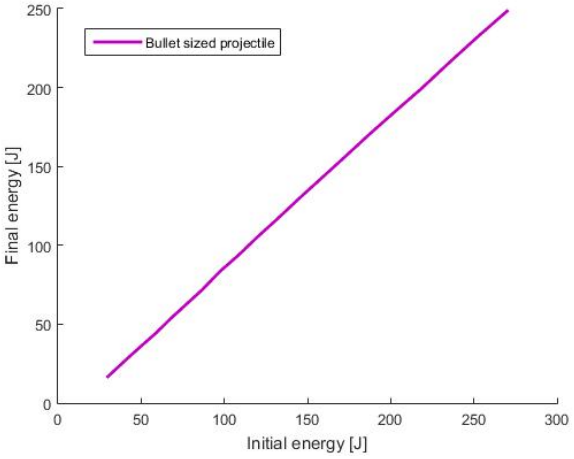

Figure 44: Final energy vs Initial energy.

As the increased mass of the bullet tears through the panel, it overcomes easily the maximum amount of energy absorbed without breaking, which was of 13 J.

7.8 Orientation of the impact

I thought it could be interesting to study how would the UHMWPE react against an oblique impact. Instead of the straight impact test, the velocity vector was slanted by a certain angle.

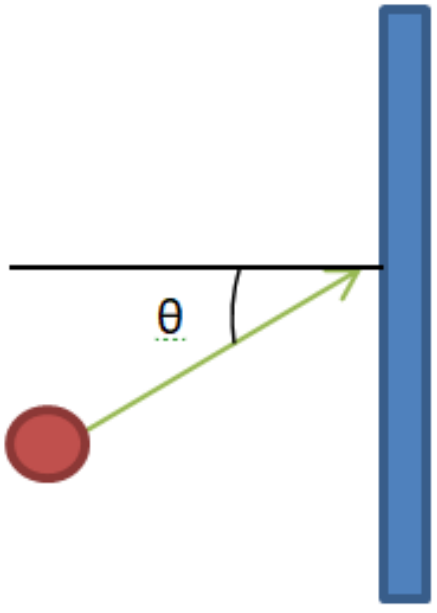

Figure 45: Angle definition.

The results shown below represent the total residual velocity of the projectile after the impact (Fig. 46) and the specific residual velocity in X direction (Fig. 47)

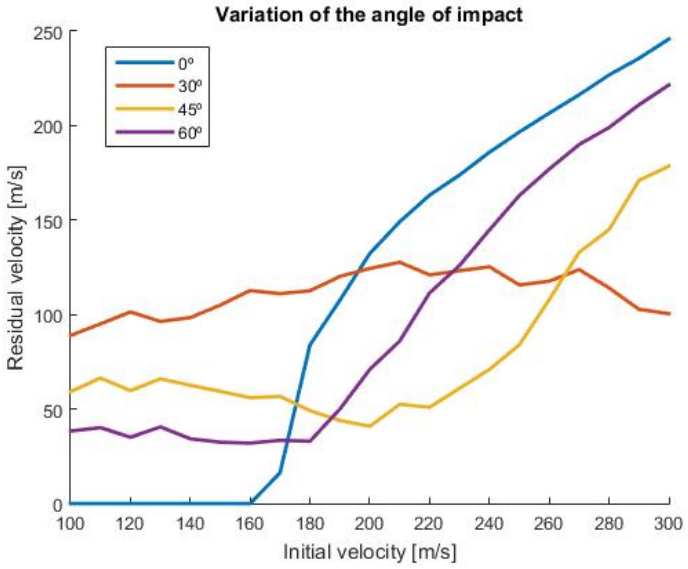

Figure 46: Residual velocity with angle variation.

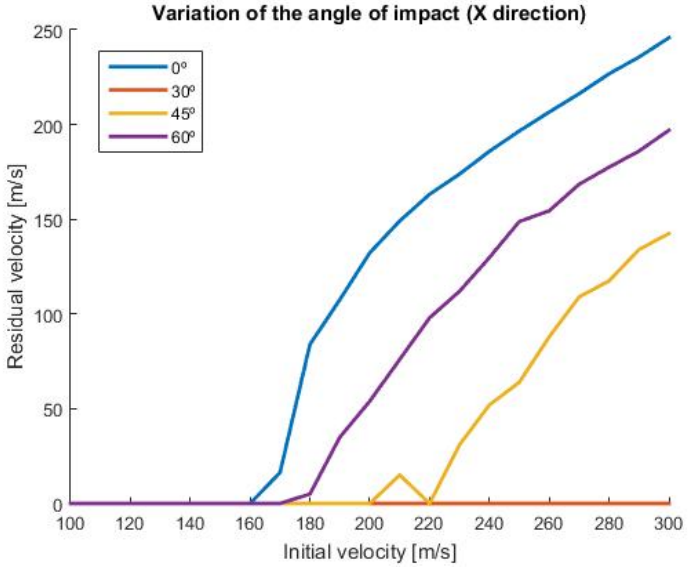

Figure 47: Residual velocity in X direction.

As it can be observed in Fig. 46, while facing an oblique impact, the material does not stop completely the bullet, but as shown in Fig. 47, the bullet does not perforate the panel until higher velocities than at the straight impact case are achieved. Instead of stopping the projectile, it bounces off after fracturing a number of plies.

The graphs of the energy absorbed while changing the angle of impact left an interesting result. Taking into account the total velocity of the projectile instead of the x directed, it can be observed how the velocity drops after breaking through a new ply.

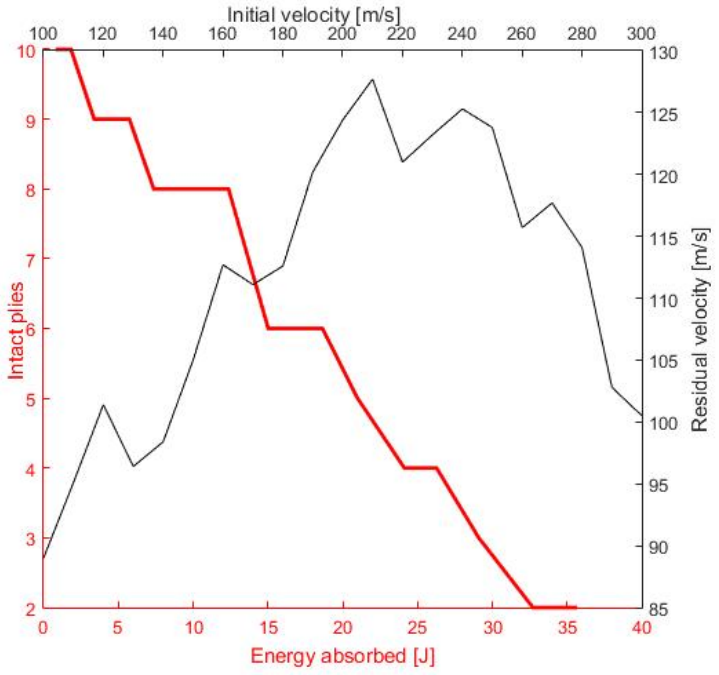

Figure 48: Energy absorbed by the system against a 30° impact.

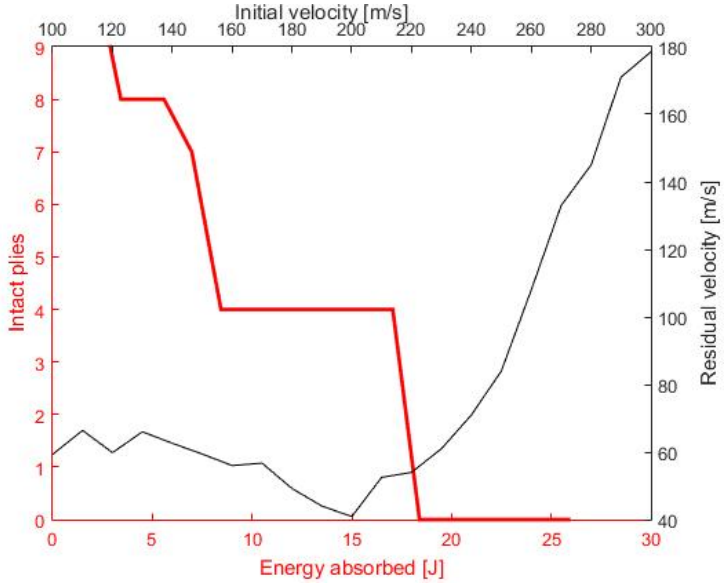

Figure 49: Energy absorbed by the system against a 45° impact.

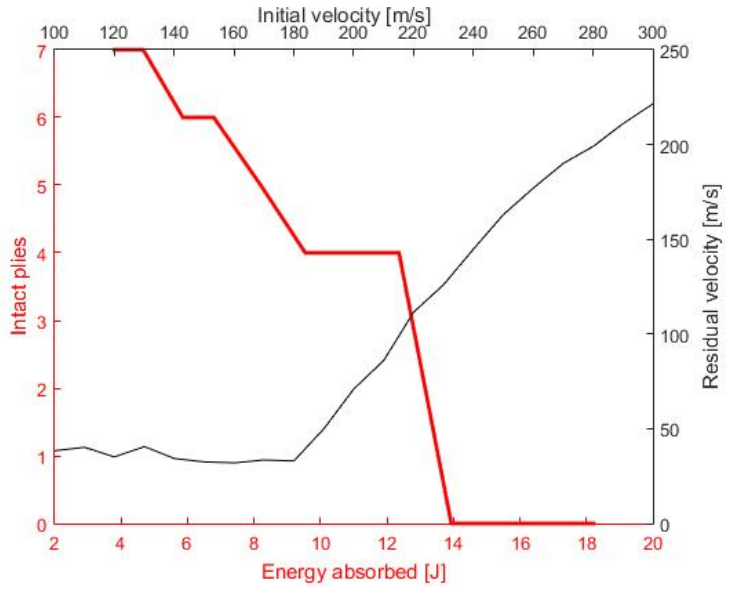

Figure 50: Energy absorbed by the system against a 60º impact.

While the projectile has not enough energy to tear through a ply, the velocity will increase until it has enough to rip through it, colliding with a fresh ply. This new ply will again absorb part of the energy after engaging with the projectile, repeating this process until the projectile has broken through all the plies or it loses all its forward speed, bouncing off the panel.

The drops in residual velocity coincide with the tearing through a new ply.

8 Conclusions & future works

The main objective of this project was to create an impact model to understand the mechanical behavior of UHMWPE against impacts. As stated before, understanding the full mechanics and physics behind the behavior of the material is well beyond the scope of this project, so it is treated as an initial step in the investigation.

8.1 Conclusions

- The model created for the simulations is accurate enough as to recreate the results from experimental tests. This would help save efforts in the creation of hard prototypes.
- The mesh has a high impact in the results obtained. A finer mesh, distributed in a more regular way can potentially offer better results. This implies that the model could benefit greatly from a mesh optimization process to obtain a
- UHMWPE has a great energy absorption, as observed from the results of the simulations.
- The panels are resilient enough as to bounce back the projectile when shot diagonally (not in a straight line). This can prove to be useful in combat scenarios, when shot under cover.

At the end of this project some facts have been learned about the mechanical behavior of UHMWPE:

- The effect of strain rate variation is linear, so two curves are enough to extrapolate the data.
- The Young modulus affects the material at low velocities because rigidity has an effect on the material.
- Increasing the velocity of the projectile affects the amount of energy it can absorb.
- The type of solid used to model the projectile has almost no effect on the results of the simulation.

One of the biggest limitations of this model is the projectile. Nowadays, no projectile is a small sphere, most projectiles have a conic section which gives it more penetrative power.

A lot more research needs to be done to check whether UD UHMWPE can fulfill the requisites to be really bulletproof.

8.2 Future works

As explained in this document, most of the material constants were extracted from previous experiments. One future line of work could be to conduct a series of experimental tests to obtain those values first hand. This way, another set of data would be generated to corroborate the validity of the work.

This project being the starting point of a wider, more in depth study, had a limited amount of parameters changed. For future investigations, other parameters, such as new projectile geometries, different projectile materials or the boundary conditions of the panel, should be changed. It could also be of interest to study a wider array of values for the parameters studied in this investigation.

To continue the investigation, the orientation of the plies forming the panel could be changed. In this project, UD UHMWPE fabric was used. This fabric was stacked into panels with the same orientation, so forming panels with varying ply stacking could be interesting.

Another future step would be the study of hybrid panels, mixing UD UHMWPE with ceramic materials, or other types of ballistic fabrics. It can also be studied how would the panel behave if the plies were glued between them.

A new set of parameters can be modified, e.g. the areal density, the size of the panel, the structure of the mesh or the thickness of each individual ply.

One of the most important points to study in this model is the projectile. A new bullet model, with the ability to represent reliably the real behavior of a bullet, could enhance the study of the panel. Creating a

model in which the bullet deforms after impact, and with two different materials in its composition could prove an interesting point.

References

[1] Wikipedia. Body armor. consulting date: August, 2017. https://en.wikipedia.org/wiki/Body_armor#Modern_use.

[2] Wikipedia. Bulletproof vest. consulting date: August, 2017. https://en.wikipedia.org/wiki/Bulletproof_vest.

[3] B.G. Falzon M. Yong, L. Iannucci. Efficient modelling and optimisation of hybrid multilayered plates subject to ballistic impact. *International Journal of Impact Engineering*, 37:605–624, 2010.

[4] Garry Wells Xiaogang Chen, Yi Zhou. Numerical and experimental investigations into ballistic performance of hybrid fabric panels. *Composites: Part B*, 58:35–42, 2014.

[5] Yuanming Xia Wen Huang, Yang Wang. Statistical dynamic tensile strength of UHMWPE-fibers . *Polymer*, 45:3729–3734, 2004.

[6] David W. Hagy Michael B. Mukasey, Jeffrey L. Sedgwick. *U.S. Department of Justice*, 2008.

[7] Everytown. Consulting date: August 2017. https://everytownresearch.org/gun-violence-by-the-numbers/#.

[8] Center for Disease Control and Protection. Consulting date: August 2017. https://www.cdc.gov/nchs/fastats/homicide.htm.

[9] Wikipedia. United states military casualties in the war in afghanistan. consulting date: August, 2017. https://en.wikipedia.org/wiki/United_States_military_casualties_in_the_War_in_Afghanistan.

[10] Wikipedia. List of afghan security forces fatality reports in afghanistan. consulting date: August, 2017. https://en.wikipedia.org/wiki/List_of_Afghan_security_forces_fatality_reports_in_Afghanistan.

[11] Abaqus 6.12 documentation. consulting date: August, 2017.

[12] Wikipedia. Bayonet. consulting date: August, 2017. https://en.wikipedia.org/wiki/Bayonet#Early_history.

[13] J.N. Reddy. *An Introduction to the Finite Element Method (Third ed.)*. McGraw-Hill, 2006.

[14] Abaqus analysis user's manual. http://abaqus.software.polimi.it/v6.12/books/usb/default.htm.

[15] David Roylance. Finite element analysis. *Department of Materials Science and Engineering*, 2001.

[16] Abaqus/cae user's manual. http://130.149.89.49:2080/v6.12/books/usi/default.htm?startat=pt06ch57s12.html.

[17] Gobierno de España. Xviii convenio colectivo nacional de empresas de ingenieria y oficinas de estudios tecnicos. *Boletín Oficial del Estado*, 2017.

[18] David W. Hagy Michael B. Mukasey, Jeffrey L. Sedgwick. Ballistic Resistance of Body Armor NIJ Standard-0101.06. July 2008.

[19] DSM. Dyneema®, with you when it matters. consulting date: August, 2017. https://www.dsm.com/products/dyneema/en_AU/home.html.

[20] Wikipedia. Ultra-high-molecular-weight polyethylene. consulting date: August, 2017. https://en.wikipedia.org/wiki/Ultra-high-molecular-weight_polyethylene.

[21] Wikipedia. 9 x 19 mm parabellum. consulting date: August, 2017. https://es.wikipedia.org/wiki/9_%C3%97_19_mm_Parabellum.

[22] William H. Cook Gordon R. Jonhson. A constitutive model and data for metals subjected to large strains, high strain rates and high temperatures. *Engineering Fracture Mechanics*, 21:31–48, 1985.

[23] Tarek Mabrouki Yancheng Zhang, J.C. Outeiro. On the selection of Johnson-Cook constitutive model parameters for Ti-6Al-4V using three types of numerical models of orthogonal cutting. *Procedia CIRP*, 31:112–117, 2015.